



Sudan University of Science & Technology



College of Petroleum Engineering & Technology

Department of Petroleum Engineering

The effect of Fracture Length and Conductivity on Well Production - Case Study Gas Field- Sudan

تأثير طول وموصلية الشق على إنتاجية الابار - دراسة حالة حقل غاز -
السودان

Presented to the college of Petroleum Engineering &
Technology for a partial fulfillment of the requirement for the
degree of B.sc of Petroleum Engineering

Prepared by:

Abbas Haider Abbas Mohammed Ali

Abd alrhman Ahmed Dafallah Mohammed

Anas Daffalla Malik Mustafa

Mojeeb Alrahman Abdelmuneim Bashier Hamid

Supervised by:

Dr. Elham Mohammed Mohammed Kahir

October 2016

The effect of Fracture Length and Conductivity on Well Production - Case Study Gas Field- Sudan

تأثير طول وموصلية الشق على إنتاجية الآبار - دراسة حالة حقل غاز -
السودان

مشروع تخرج مقدم إلي كلية هندسة وتكنولوجيا النفط - جامعة السودان للعلوم
والتكنولوجيا

إنجاز جزئي لأحد المتطلبات للحصول على درجة بكالوريوس العلوم في هندسة
النفط

إعداد الطلاب:

عباس حيدر عباس محمد علي

عبد الرحمن احمد دفع الله محمد

أنس دفع الله مالك مصطفى

مجيب الرحمن عبد المنعم بشير حامد

تمت الموافقة على هذا المشروع من كلية هندسة وتكنولوجيا النفط

المشرف على المشروع :

د. الهام محمد محمد خير

..... التوقيع :

رئيس قسم هندسة النفط :

أ. فاطمة أحمد التجاني

..... التوقيع :

عميد كلية هندسة وتكنولوجيا النفط :

د. تقوى أحمد موسي

..... التوقيع :

التاريخ : / / 2016

بسم الله الرحمن الرحيم

الاستهلال

قال تعالى:

(يعلم ما بين أيديهم وما خلفهم ولا يحيطون به علما)

سورة طه (١١٠)

DEDICATION

*This work is dedicated
To the people who helped and
supported us in all aspects of life;*

*Our parents
To those who stand by our side during the whole
journey;*

*Our brothers & sisters
To those who gave us a lot of lessons to learn, and
inspired us to get involved in a beautiful world of
science,*

*Our teachers
To those who have a hand in this success
Our friends*

AKNOWLEDGMENTS:

*First of all; we would like to thank God for his blessing on us to
achieve this work.*

*Secondly; we would like to give many thanks to the castle of
science Sudan university of science & technology; as well as college
of petroleum engineering & technology generally, and
department of petroleum engineering especially.*

*We would like to express our sincere appreciation to our
supervisor **Dr. Elham Mohammed Mohammed
Kahir** for her guidance, inspiration, and assistance. In addition;
for her wisdom and authoritative knowledge. That has upper
hand in accomplishing the research in its current view.*

*We also want to give special thanks to the staff of SUDAPET and
the Ministry of Petroleum and Gas for their contribution in our
work.*

Abstract

Hydraulic fracture is a well stimulation technique in which a pressure-induced fracture to form a conductive path for trapped fluids in low permeable zone; it is also applied to unconsolidated high permeable zone to control the movement of formation sand toward the wellbore. The production through this fracture is a function of two factors, fracture length and conductivity. Through this study, the effect of fracture length and conductivity in gas production and cumulative gas production was presented for a gas well in Block 8. The Block is 200 km Southeast of Khartoum and it covers an area of 60,000 km²; It is sandy shale block with gas in place of 5.2 MMM ft³; only two vertical wells were drilled in the block.

Series of scenarios were implemented for different fracture lengths and conductivities using the default shaly sand properties combined with advance reservoir simulator program (Computer Modeling Group - CMG). Six different values of fracture conductivity (1, 2, 3, 4, 5, and 10) and five different fracture lengths (300, 500, 700, 900, and 1000 ft) were studied; with constant fracture width of 0.05 ft.

The results presented that the optimum fracture conductivity and fracture length is 100 ft increase the $q_{g,0}$ and length of 1000 ft respectively; a fracture conductivity of 1 and recovery factor from 0.82% to 3.32% with a daily gas production of 43856 ft³/day, while the bbl of water. The cumulative gas was reached 0.6 MMM ft³ with

The optimization of fracture length and conductivity in this study were based only on gas production rate, water production rate and the cumulative production during the the net present value because no simulation time; the optimization did not considered information was available for the costs.

Key Words

Hydraulic Fracturing; Fracture Conductivity; Fracture Length; Gas Production; Optimization.

التجريد

التشقيق الهيدروليكي هو تقنية تحفيز للأبار والتي يتم فيها استخدام ضغط لعمل شق لتوصيل موائع المكامن منخفضة النفاذية؛ ويتم تطبيقه أيضا على مناطق النفاذية العالية غير المتماسكة للسيطرة على حركة رمال الطبقة نحو حفرة البئر. وإنتاج من خلال خذخ الشقوق يعتمد على عاملين هما طول وموصلية الشق. خلال هذه الدراسة، تم عرض تأثير طول وموصلية الشق على معدلات الإنتاج والإنتاج التراكمي للغاز للبئر غازي في مربع ٨. وبعيد هذا المربع مسافة ٢٠٠ كيلومتراً جنوب شرق الخرطوم ، وهو يغطي مساحة قدرها ٦٠,٠٠٠ كيلومتراً مربعاً . وهو ذو طبيعة رملية طينية تحتوي على كمية من الغاز تقدر بحوال ٥,٢*١٠^٩ قدماً مكعباً. وقد تم اسكتشاف بئرين فقط من ابار الغاز العمودية في الحقل.

تم تنفيذ سلسلة من السيناريوهات لاطوال وموصليات شق مختلفة باستخدام خصائص الرمل الطيني الافتراضية مع برنامج محاكاة المكامن (مجموعة النمذجة بالكمبيوتر). تمت دراسة ست قيم مختلفة لموصلية الشق (١، ٢، ٣، ٤، ٥، ١٠) وخمسة أطوال مختلفة للشق (٣٠٠، ٥٠٠، ٧٠٠، ٩٠٠، ١٠٠٠ قدم). مع عرض شق ثابت يبلغ ٠,٥ قدم.

اظهرت النتائج أن أمثل شق هو شق بطول ٩٠٠ قدم وموصلية مقدارها ٢,٠. بهذه الموصلية والطول حدثت زيادة في معامل الاستخلاص من ٠,٨٢٪ إلى ٣,٣٢٪ مع إنتاج يومي للغاز بمقدار ٤٣٨٥٦ قدماً مكعباً/يوم، بينما بلغ الغاز التراكمي ٦,٠*١٠^٨ من الاقدام المكعبة مع ١٢٨٢٨ برميل من الماء.

واستند الاختيار الأمثل لطول وموصلية الشق في هذه الدراسة فقط على معدل إنتاج الغاز، ومعدل إنتاج المياه والإنتاج التراكمي خلال فترة المحاكاة. ولم يؤخذ في الحسبان صافي القيمة الحالية لأنه لا تتوفر المعلومات الكافية عن تكاليف المواد المستخدمة في عملية التشقيق.

الكلمات المفتاحية

التشقيق الهيدروليكي؛ موصلية. طول الشق، إنتاج الغاز؛ أمثلية

Nomenclature:

	SE	South East direction
	MD	Measured Depth
	E logs	Electric logs
	Ppm	Parts per million
	TD	Total Depth
PVT analysis		Pressure-Volume-Temperature analysis
WNPOC		White Nile Petroleum Operating Company
	RCS	Resin-coated sand
	ISP	Intermediate-strength proppant
	LWP	Light-weight proppant
CR		Dimensionless fracture conductivity
F _{CD}		Dimensionless fracture conductivity
	L _f	Fracture half-length
	W*k _f	Fracture conductivity
	K:	Formation permeability
	K _f :	fracture permeability
	π	Constant = 3.1416
ΔG _p		The incremented gas production
ΔL _p		Incremental propped fracture length
	ΔV _{ft}	Volumes of fracture fluid
		Created fracture length ΔL _c
	X _f	Optimal fracture half-length
X _e , Y _e		Rectangular reservoir dimensions
	V _p	Proppant volume
	h	Formation thickness
	φ _f	Fracture porosity
	P3D	Pseudo 3D models

	NPV	Net Present Value
	PDA	Production Data Analysis
	PTA	Pressure Transient Analysis
	RPI	Reciprocal Productivity Index
	PBU	Pressure Transient Build Up
	GPA	Gas Production Analysis
	Fnd	Non-Darcy conductivity multiplier
F_{CDcri}		Critical dimensionless fracture conductivity
	W_f	Fracture width
	X_{df}	Designed fracture half length
	X_{fa}, X_{app}, L_{xa}	Apparent fracture half length
Q_{DA}		Dimensionless cumulative production based on area (A)
	P_{wD}	Dimensionless wellbore pressure
	t_a	Pseudo equivalent time, days
t_{DA}		Dimensionless time based on area (A)
C_{TD}		Dimensionless Fracture Conductivity
	\emptyset	Porosity fraction
	C_t	Total compressibility
	$L_{xf}, X_{created}$	Fracture half-length
k_f		Effective permeability to gas in the fracture
		Density ρ
		Viscosity μ
	v	Superficial fluid velocity cm/s
	β	Forchheim initial coefficient

PKN	Perkins-Kern-(Nordgren) model
GDK	Kristianovich - Zheltov - (Gertsmaa - DeKlerk) model
CMG	Computer Modeling Group
Pb	Bubble point pressure
PI	Productivity Index
FE	Flow Efficiency
AOF	Absolute Open Flow rate
GOIP	Original gas in place
BHP	Bottom Hole pressure
LGR	Local Grid Refinement
ZD	Z Direction

List of contents:

.....	الاستهلال	i
Dedication.....		ii
Acknowledgments.....		iii
Abstract.....		vi
.....	التجريد	v
Nomenclature.....		vii
List of contents.....		ix
List of figure.....		xi
List of tables.....		xiii
Chapter 1 General Introduction.....		1
1.1 Introduction.....		2
1.2 General informations about the field.....		3
1.3 Problem statement.....		5
1.4 Study objectives.....		5
Chapter 2 Theoretical Background and Literature Review.....		6
2.1 Theoretical Background.....		7
2.1.1 Fracturing fluids.....		8
2.1.2 Proppants agents.....		10
2.1.3 Fracture conductivity.....		10
2.2 Literature review.....		11
Chapter 3 Methodologies and Procedures.....		32
3.1 Global (Parent) Grid.....		33
3.2 Reservoir Rock and Fluid Properties.....		34
3.3 History Match.....		37
3.4 Local Grid Refinement.....		41

3.5 Optimization of Fracture Length and Conductivity.....	42
Chapter 4 Results & Discussion.....	44
4.1 Optimum length selection.....	45
4.2 Optimum conductivity selection.....	49
Chapter 5 Conclusion & Recommendations.....	52
References.....	54

List of figures:

Figure 1.1: Location map of block8.....	3
Figure 2.1: Chemicals Used in Hydraulic Fracturing Fluids.....	9
Figure 2.2: Description of Effective Fracture Length	14
Figure 2.3: Optimum fracture length for that particular proppant volume.....	22
Figure 2.4: Fracture length versus different fracture permeability.....	23
Figure 2.5: Fracture pressure history match using production analysis	23
Figure 2.6: A comparison of effective fracture half-lengths computed from PDA....	25
Figure 2.7: Comparison of effective half-lengths from numerical reservoir modeling and PTA versus design fracture half length.....	26
Figure 3.1: Schematic Diagram for Formation and Sub- layers for the Model.....	36
Figure 3.2: The Location of well Hosan -1.....	37
Figure 3.3: Gas Production History Match Plots of Hosan 1.....	38
Figure 3.4: The Bottom Whole Pressure History Match Plots of Hosan 1.....	39
Figure 3.5: 3D Viewer of Permeability Distribution at the Beginning of Simulation.....	40
Figure 3.6: 3D Viewer of Gas Saturation Distribution at the Beginning of Simulation.....	40
Figure 3.7: 3D Viewer of Pressure Distribution at the Beginning of Simulation.....	41
Figure 3.8: 3D Viewer showing Parent Grid and Child Grid of the LGR Model....	42
Figure 4.1: Cumulative gas production for conductivity 5 for different fracture lengths.....	45
Figure 4.2: Cumulative water production for conductivity 5 for different fracture lengths.....	46

Figure 4.3: Gas production rate for conductivity 5 for different fracture lengths.....47

Figure 4.4: Water production rate for conductivity 5 for different fracture lengths.....48

Figure 4.5: Cumulative gas production for L=700 ft for difference dimensionless fracture conductivities (C_D).....49

Figure 4.6: Cumulative water production for L=700 ft for difference dimensionless fracture conductivities (C_D).....50

List of tables:

Table 3.1: PVT Correlation.....	34
Table 3.3: Gas PVT Properties.....	35
Table 3.3: The available Well Test Results.....	36
Table 4.1: Changing cumulative gas and water production according to difference lengths.....	48
Table 4.2: Changing cumulative gas and water production according to difference conductivity.....	51
	Dimensionless

CHAPTER 1

GENERAL INTRODUCTION

Chapter 1

General Introduction

1.1. Introduction

With the first experiments done in 1947, and the first industrial use in 1949. The technology of hydraulic fracturing for hydrocarbon well stimulation has been used since then for reservoir stimulation and enhanced hydrocarbon recovery. Hydraulic fracture is a pressure-induced fracture caused by injecting fluid into a target rock formation. Fluid is pumped into the formation at pressures that exceed the fracture pressure. The pressure at which rocks break. To access a zone for stimulation, engineers perforate the casing across the interval and use retrievable plugs to isolate the interval from other open zones. This interval is then pressurized to the formation breakdown pressure, or fracture initiation pressure, the point at which the rock breaks and a fracture is created.

The wings of the fracture extend away from the wellbore in opposing directions according to the natural stresses within the formation. Proppant, such as grains of sand of a particular size, is mixed with the treatment fluid to keep the fracture open when the treatment is complete. Hydraulic fracturing creates high-conductivity communication

with a large area of formation and bypasses any damage that may exist in the near-wellbore area.

The Physics of Fracturing, The size and orientation of a fracture, and the magnitude of the pressure needed to create it, are dictated by the formation's in situ stress field. This stress field may be defined by three principal compressive stresses, which are oriented perpendicular to each other. In situ stresses control the orientation and propagation direction of hydraulic fractures. Hydraulic fractures are tensile fractures, and they open in the direction of least resistance. The hydraulic fracture will alter the flow into the wellbore from radial to linear flow.

Parker *et al.* (1994) state that the Hydraulic fracturing is an established technique for stimulation of the production in low-permeability reservoirs and for bypassing damage in moderate- permeability reservoirs. Hydraulic fracturing has recently been applied to high-permeability formations to bypass completion damage and actually stimulate production.

1.2. General Information about the Field

Block-8 which is situated in the eastern central Sudan it is around 300 km SE Khartoum. It is covers an area of 60,000 km² Fig 1.1. It is within the vicinity of Al-Jebalain Export Pipeline and crossed by a variety of transportation networks. No high relief or exposures, the area is flat bounded by the Blue Nile from the west and dissected by the Dinder, Rahad rivers and their tributaries, the area average elevation is 400 m above the sea level. Most of it is covered by Tertiary/Quaternary sediments (Gezera and Umrwaba formations).

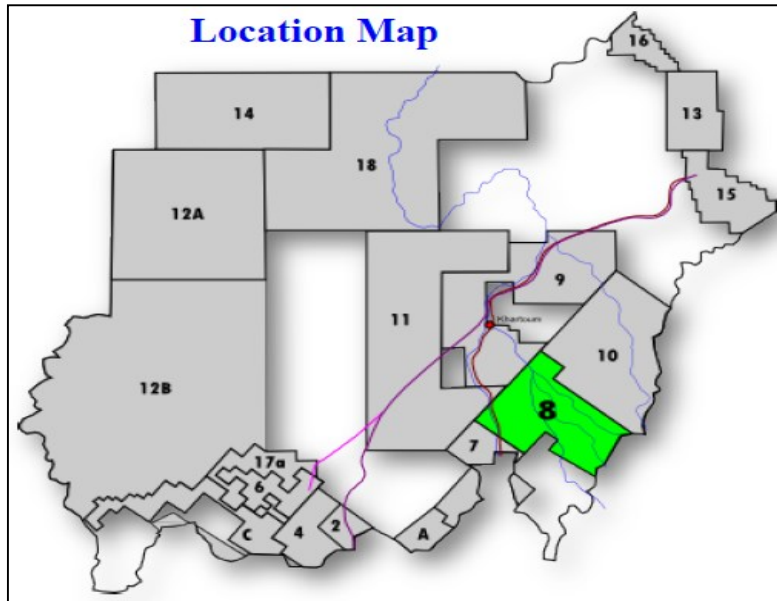


Fig 1.1 Location Map of Block 8

The block is covered Blue Nile Basin of Sudan; and it consist of three main Sub-basins. Dinder I, Dinder II and Dinder III Dinder I formation is demarcated at 508m MD from E logs. This formation consists mainly of fine to medium grained sandstone. Coarse grained are observed in this section as well. It is moderately to poorly sorted. The clay stone is soft to firm, silty and sandy, varicolored, commonly reddish-brown to greenish grey and yellowish white. The base of this formation which lies uncomfortably with the top of Dinder II formation. This section is about 639 meters thick. No hydrocarbon shows are observed in the cuttings.

Dinder II Formation top is derived at 1147m MD based on E logs. This formation comprises intercalated sand stone, clay stone and thin layers of siltstone. There is cycling in sandstone dispositioning indicating high and low current environment and repeating of depositional periods. Rare pyrite is observed in the cutting samples. The clay stone is oxidized Belo the unconformity of the formation top. It is predominantly reddish brown in colour, minor is light to medium grey while becoming dark with depth towards the base of the formation. It is also silty, and in part sandy. No oil stain is observed in the cuttings. A high peak of total gas (143,048 ppm, 14.3%) is recorded in Lower Dinder II formation at 1827.5 m MD. The sequence thickness is about 725 meters.

Dinder III Formation top is defined at 1872m MD based on E logs. This sequence is dominated by inter bedded sandstone and clay stone with minor siltstone. The

sandstone is commonly fine to very fine in grain size. it is poorly calcareous cemented. Thin stringers of siltstone less than two meters in thickness are also observed. The siltstone is off white grey to greenish grey in colour, poorly calcareous cemented and firm to moderately hard. The clay stone is predominantly reddish brown in colour while minor are light to medium grey. It is silty and sandy and moderately hard. Rare pyrite is also observed in the cuttings. Poor oil shows are recorded throughout this section in the sand and thin stringers of siltstone. No oil stain no primary fluorescence is observed, while only very slow milky white streaming cut fluorescence with no residual ring is observed. Dinder III thickness is about 808 meters. Dinder III and Blue Nile reservoir may contain lighter oil than in Dinder 2 reservoir. But it is also highly possible that

natural gas accumulated in the structure

Total of six wells have been drilled in this Block. The sources rock analysis carried out so far suggest a more gas-prone source. However, this is in no way conclusive in such that samples analyzed may not represent the whole Basin. Evidence to this is the good indication of elevated type II Kerogen in Hosan-1 samples. Trap presence and effectiveness is the major challenge in exploring this Block; not that traps are not present, but they are rather difficult to identify and map properly. Complication of interpretation and mapping is caused mainly by the complexity of the structural setting of this Basin.

Hosan-1 is the first well drilled in Block 08, the well is wildcat well with TD of 2911.0 meters on 23rd Jan 2005 to test the petroleum potentiality of Prospect gas in place, the well will also be expected to penetrate the optimum location of the pinch-out of the Blue Nile Formation. It was plugged back to 1688 meters. The well location is 12.67 km south-west of Dinder-1 well. No oil shows observed while drilling, Gas shows is being measured by the Data log Chromatograph. The well testing was performed during the period between 16th Nov to 6th Dec 2008. No down-hole gas sample collected for a full PVT analysis for Hosan-1, only surface gas sample is collected and gas chromatograph analysis has been done. No core recovery from this well, the permeability estimated from the log and within the range of the Well test result. Most of the drilled wells are off structures.

The primary objectives of Hosan-1 are the Dinder 3 sands and Lower Dinder 2 sands, and the secondary objectives are the Blue Nile sands, the Upper Dinder 2 sands and the shallow Dinder 1 sands which are oil bearing in Dinder-1 well. The well location selected is considered optimum to penetrate all the targeted zones with

emphasis on the primary targets. In Dinder-1 well, overpressure was encountered from Lower Dinder 3 sand downward. Similar overpressure zone may also exist in Hosan-1, which may assist in maintaining the porosity up to 25.6% at 3000m and 17% at 3625 m as seen in Dinder-1 well.

1.3. Problem Statement

Hydraulic fracture was presented as a unique technique for the production of hydrocarbon from Unconventional hydrocarbon recourses such as shale gas; the optimization of the fracture parameters such as fracture conductivity and Fracture length is the major factor for a favorable fracture job. White Nile Petroleum Operating Company WNPOC discovered significant amounts of dry, non-associated natural gas in block eight. More than 100,000 ppm gas readings encountered during the drilling operations in shale gas. No work was conducted before for the study of the effect of fracture in the field recovery; however, this study presented parameters the effect of fracture length and conductivities on well production for a gas well in Block 8 (Hosan-1).

1.4. Study Objectives:

The main objective of this study is to analyze the effect of fracture on well productivity for low permeable zone in Block 8 in Sudan. Based on gas and water flow rates and the cumulative production for a particular time and without considering the Net present Value for the fracture job, optimization of fracture parameters was presented through the work; which included:

1. Analysis and optimization of the best fracture half-lengths.
2. Analysis and optimization of the best fracture conductivities.

CHAPTER 2

THEORETICAL BACKGROUND AND LITERATURE REVIEW

Chapter 2

Theoretical Background and Literature Review

2.1 Theoretical Background

At the surface, a sudden drop in pressure indicates fracture initiation, as the fluid flows into the fractured formation. To break the rock in the target interval, the fracture

initiation pressure must exceed the sum of the minimum principal stress plus the tensile strength of the rock. To find the fracture closure pressure, engineers allow the pressure to subside until it indicates that the fracture has closed again. Engineers find the fracture reopening pressure by pressurizing the zone until a leveling of pressure indicates the fracture has reopened. The closure and reopening pressures are controlled by the minimum principal compressive stress. Therefore, induced down hole pressures must exceed the minimum principal stress to extend fracture length. After performing fracture initiation, engineers pressurize the zone for the planned stimulation treatment. During this treatment, the zone is pressurized to the fracture propagation pressure, which is greater than the fracture closure pressure. Their difference is the net pressure, which represents the sum of the frictional pressure drop and the fracture-tip resistance to propagation. Keeping Fractures Open the net pressure drives fracture growth and forces the walls of the fracture apart, creating a width sufficient to allow the entry of the fracturing slurry composed of fluid and proppant solids that hold the fracture open after pumping stops. Once the pumping is halted, the pressures inside a fracture subside as the fluids either flow back into the well or leak away into the reservoir rock. This drop in pressure allows the fracture to close again. To ensure that fractures stay open, engineers inject additional materials, depending on lithology. In sandstone or shale formations, they inject proppant sand or specially engineered particles—to hold fractures open (below). In carbonate formations, they pump acid into the fractures to etch the formation, creating artificial roughness. The stimulation treatment ends when the engineers have completed their planned pumping schedule or when a sudden rise in pressure indicates that a screen out has taken place. Controlling Hydraulic Stimulation engineers maintain a constant rate of fluid injection. The volume injected includes the additional volume created during fracturing and the fluid loss to the formation from leak off through the permeable wall of the fracture. However, the rate of fluid loss at the growing fracture tip is extremely high. Therefore, it is not possible to initiate a fracture with proppant in the fracturing fluid because the high fluid loss would cause the proppant at the fracture tip to reach the consistency of a dry solid, causing bridging and screen out conditions. Consequently, some volume of clean fluid a pad must be pumped before any proppant is pumped. When designing a hydraulic fracture treatment, engineers must establish the leak off rate and volume of the pad in relation to the timing of slurry and proppant injection so that when the fracture reaches its designed length, height and width, the first particle of proppant reaches the fracture tip. The fracture into

preferred zones or to halt the treatment before the fracture grows out of the intended zone. The propagation of hydraulic fractures obeys the laws of physics. In situ stresses control the pressure and direction of fracture initiation and growth. Engineers carefully monitor the stimulation process to ensure it goes safely and as planned (Schlumberger 2013).

2.1.1 Fracturing Fluids

Fracturing fluids are liquids or gases that convey pressure from the surface into the reservoir to enable fractures to be created. Fracturing fluid allows transportation of proppant and chemicals into the reservoir. The choice of hydraulic fracturing fluid is dependent on the properties within the Reservoir and most common types are:

I. Water-based fluids:

Water is the most common base fluid used in hydraulic fracturing due primarily to the low cost and availability.

II. Foam-based fluids:

Foams are structured, two-phase fluids that are formed when a large internal phase volume (typically 55 to 95%) is dispersed as small discrete entities through a continuous liquid phase.

III. Oil-based fluids:

Oil-based fracturing fluids were the first high-viscosity fluids used in hydraulic fracturing operations.

IV. Acid-based fluids:

The main difference between acid fracturing and proppant fracturing is the way fracture conductivity is created. In proppant fracturing, a propping agent is used to prop open the fracture after the treatment is completed. In acid fracturing, acid is used to “etch” channels in the rock that comprise the walls of the fracture. Thus, the rock must be partially soluble in acid so that channels can be etched in the fracture walls.

V. Alcohol-based fluids:

Some companies used methanol as a base fluid in fracturing applications in Canada and Argentina. In those cases, the fractured formations either had low permeability with high clay content and low bottom-hole pressure.

VI. Emulsion-based fluids:

An emulsion a mixture of two or more liquids that are normally immiscible is used as the fracturing fluid. There are many different emulsion-based fluids that have

been developed and used as fracturing fluids. Many of such fluids use emulsions of oil and water, and could therefore be classified under the oil-based fluids.

VII. Cryogenic fluids (CO₂, N₂, He, etc.):

The family of these fluids consists of pure liquid CO₂ and a binary fluid consisting of a mixture of liquid CO₂ and N₂ to reduce costs. To make fluids suitable for hydraulic fracturing, chemicals are commonly added to create a highly viscous low friction fluid that will withstand the rigors of traveling to the zone of interest, readily carry the proppant material into the fractures and ultimately return to surface. The number of chemicals and concentrations added to the fluid/proppant mixture is highly variable and dependent on the specific properties of the reservoir.

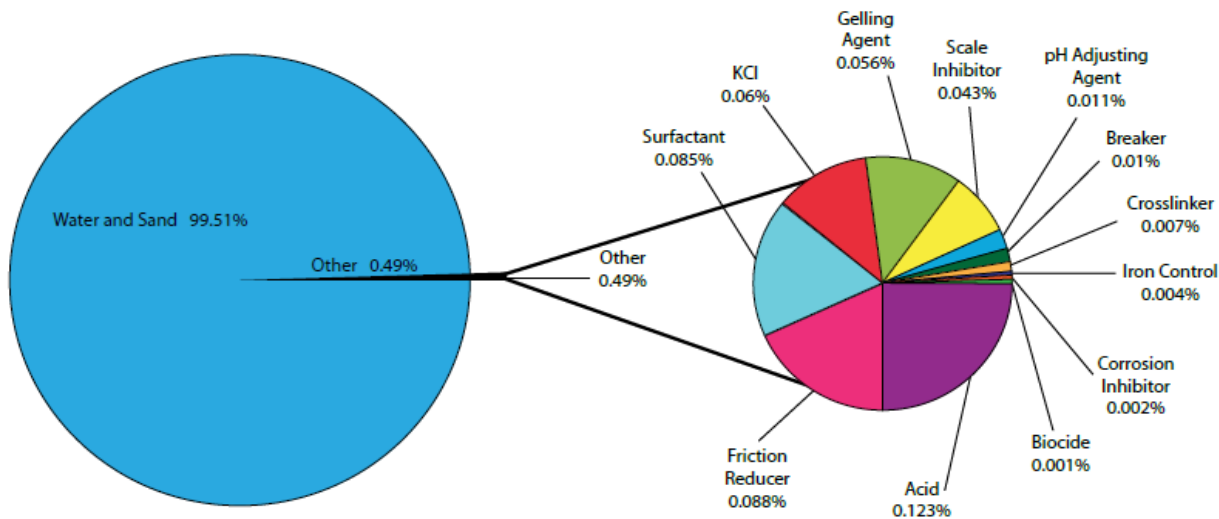


Fig 2.1 Chemicals Used in Hydraulic Fracturing Fluids.

2.1.2 Proppants Agents:

Propping agents are required to "prop open" the fracture once the pumps are shut down and the fracture begins to close. The ideal propping agent is strong, resistant to crushing, and resistant to corrosion, has a low density, and is readily available at low cost (Holditch 1979). The products that best meet these desired traits are silica sand, resin-coated sand (RCS), and ceramic proppants.

Silica sand is optimum to be tested to be sure it has the necessary compressive strength to be used in any specific situation. Generally, sand is

used to prop open fractures in shallow formations. Sand is much less expensive per pound than RCS or ceramic proppants. RCS is stronger than sand and is used where more compressive strength is required to minimize proppant crushing. Some resins can be used to form a consolidated pack in the fracture, which will help to eliminate proppant flow back into the wellbore. RCS is more expensive than sand, but it has an effective density that is less than sand.

Ceramic proppants consist of:

- Sintered bauxite
- Intermediate-strength proppant (ISP)
- Light-weight proppant (LWP)

The strength of a ceramic proppant is proportional to its density. Also, the higher-strength proppants, like sintered bauxite, cost more than ISP and LWP. Ceramic proppants are used to stimulate deep (> 8,000 ft.) wells where large values of in-situ stresses will apply large forces on the propping agent.

2.1.3 Fracture Conductivity:

The fracture conductivity is the product of propped fracture width and the permeability of the propping agent. The permeability of all the commonly used propping agents (sand, RCS, and the ceramic proppants) will be 100 to 200 + Darcies when no stress has been applied to the propping agent. However, the conductivity of the fracture will be reduced during the life of the well because of:

- Increasing stress on the propping agents
- Stress corrosion affecting the proppant strength
- Proppant crushing
- Proppant embedment into the formation
- Damage resulting from gel residue or fluid-loss additives

The effective stress on the propping agent is the difference between the in-situ stress and the flowing pressure in the fracture. As the well is produced, the effective stress on the propping agent will normally increase because the value of the flowing bottom-hole pressure will be decreasing (Petrowiki).

2.2 Literature Review

Maimona Washie (2012) made a Geochemical evaluation carried to evaluate the source rock in Abu Gabra, pyrolysis analysis results of 617 geochemical rock samples from Azraq wells and 337 geochemical rock samples from Neem wells, used to evaluate

the richness of source rock (TOC), kerogen type (HI, S2) and thermal maturity (Tmax). VRo readings of 119 rock samples from Azraq wells and 73 geochemical rock samples from Neem wells used to measure the thermal maturity. Based on the main key parameters used to evaluate shale gas in Marine basins there is high feasibility of shale gas in Lacustrine basin.

Elham Khair, Zhang Shicheng and Zhuang Zhaofeng (2014) presented evaluation of the local Sudanese guar gum with respect to fracturing fluid. A series of standard laboratory tests were performed for the first time to address the performance of the guar gum itself and the fluid prepared with different concentrations of guar and different additives at different temperature and shear rates. The fluid exhibits a good stability with time at 65 °C; also high returned permeability was obtained when the fluid was used to saturate core samples obtained from different wells in Fulla North Oilfield in Sudan.

Elham Khair and Muhammad Farid (2016) conducted a Preliminary Evaluation of Silica Sand in Sudan with Respect to Fracture Sand. Three samples were collected from different areas in Sudan and a series of laboratory tests were performed according to the API recommended practice API RP 19C. More than 10% of fine has been produced from the different samples under stress of 3000 Psi; which indicate that the sample can be used as proppant for reservoir with the closer pressure less than 3000 Psi; for pressure above 3000 Psi, the samples have to be coated for strength improvement.

Parker *et al.* (1994) state that the Hydraulic fracturing is an established technique for stimulation of the production in low-permeability reservoirs and for bypassing damage in moderate- permeability reservoirs. Hydraulic fracturing has recently been applied to high-permeability formations to bypass completion damage and actually stimulate production. Formation fines control in poorly consolidated formations may also be a benefit from hydraulic fracturing. The hydraulic fracture will alter the flow into the wellbore from radial to linear flow. The pressure drop for production will be distributed over the created surface area of the fracture and will not be limited to the surface area of the wellbore or gravel pack radius. This distributed pressure drop will reduce flow rates per unit area, which will reduce flow velocity which should reduce formation fines movement or production. The lower flow rate over a greater surface area may actually result in higher production rates for the well. High permeability formations are not usually the realm of hydraulic fracturing. However, recently there has been a resurgence of Interest in stimulating these reservoirs. Reasons for the interest include fracturing past damaged zones, controlling and preventing sand production, and generally providing better control over the wellbore (Hunt and Soliman 1994).

Operationally, fracturing high permeability formation is different from fracturing low permeability formations due to the expected high leak-off rate, which influences fracturing pressure as a function of time. In addition, because of the desired high fracture conductivity, the concept of tip screen-out is applied (Hunt and Soliman 1994).

In tip screen-out, the fracture is designed in such a way that by the time the fracture reaches the desired length, the leading pad volume has leaked off into the formation. After the pad volume has leaked off, the presence of the proppant-laden fluid at the leading edge of the fracture inmates the screen-out process. Continued injection of the proppant laden fluid causes the fracture to widen or balloon (Smith, Miller and Haga 1987).

Hunt and Soliman (1994) results state that: Fracturing of damaged, high permeability formations should increase production and change the expected pressure profile in the formation, possibly preventing sand production. Thus, fracturing is a viable completion option for high permeability formations where wellbore damage and/or the potential for sand production exists.

When fracturing a high permeability formation, the fracture should be designed to extend beyond the external radius of the damaged region. Fractures that fail to extend beyond the damaged region will not improve production to optimum levels and will not significantly decrease the potential for sand production. It is unnecessary to generate significant fracture length beyond the external radius of the damaged region. However, it is always prudent to include a safety factor in the fracture design.

To properly design a fracture treatment it is important to run a pre-frac well test to determine formation permeability, amount of wellbore damage, and extent of wellbore damage. These parameters determine the necessity of a fracture, and optimum length and conductivity of the fracture. When fracturing a high permeability formation, a minimum fracture conductivity is required to improve production and decrease pressure drop in the formation. Generally, high fracture conductivities are desired to minimize pressure drop and gradient within the reservoir during production.

Fracture conductivity may decline during production. Therefore, to assure that production improvement is maintained and sand production is minimized over the life of the well, the initial conductivity should be greater than the minimum required to improve production and decrease pressure drop in the formation. Fracture damage limits production improvement and increases the pressure drop and gradients, however, the degree of fracture damage must be severe before a pronounced effect is detected.

Permeability reduction in the near-fracture vicinity must be great or damage must penetrate deep into the formation before a significant decline in production improvement and a pronounced pressure drop result. Deep damage away from the fracture can be minimized by properly designing the frac-pack treatment.

During production, the majority of the reservoir fluid will enter the part of the fracture outside the damaged region when the fracture extends beyond the damaged region. The topic of how to optimize fracture half-length has been discussed at length in the Petroleum Literature since the 1970s (Wei and Holditch 2009).

Effective fracture lengths are frequently observed to be much less than anticipated fracture lengths. This is seen in lower than expected production or evidenced in pressure transient analysis results. A precursor to the poor fracture performance is poor recovery of the fracturing fluid; often less than 50% is recovered during clean-up. In many reservoirs this unrecovered fracturing fluid remains immobile within the formation creating an obstruction to flow. This significantly compromises effective frac length and results in decreased production. During the fracturing process and subsequent closure of the fracture, the bulk of the fracturing fluid invades the reservoir matrix along the fracture face, referred to as the “invaded zone”. This fluid is forced into the reservoir by the significant pressure differential between fracturing pressure and reservoir pressure. Once in the matrix, removal of fluid from the invaded zone can be very difficult as it is held by relative permeability, irreducible saturation, and/or capillary pressure effects (Tudor, Nevison, and Allen 2009).

The science of hydraulic fracturing has predominately been focused on fracture geometry and proppant placement to maximize production rates and cumulative production. Current technology for hydraulically fracturing tight reservoirs, including shales, often focuses on complex fracture volumes rather than bi-wing geometry to create and maximize the formation stimulated area. This in turn results in optimized commercial production rates. Within the conventional bi-wing hydraulic fracturing theory it is well understood that the optimized fracture length is inversely proportional to reservoir permeability. Similarly, the created fracture volume model used on shales tends to follow the same theory that optimized created volume is inversely proportional to the reservoir permeability. Both conventional bi-wing and the created volume fracturing theories require that the fracture matrix be a substantial distance from the wellbore. Both theories require a conductive path from the fracture network to the

wellbore. The fracture length or volume needs to fully contribute to achieve maximum production (Tudor, Nevison, and Allen 2009).

In the practice of bi-wing fracturing theory it is well understood that the created fracture length does not always fully contribute to production. Post fracture pressure transient analysis of bi-wing fracture treatments have demonstrated and measured that the “effective fracture length” that is contributing to production is often a fraction of the created fracture length. The difference between effective fracture length and the created fracture length is missed opportunity for incremental production. Effective fracture lengths have been observed to be as low as 30% of the created fracture length (Pridie, 2009). The below Figure is a simplified diagram illustrating created and effective fracture lengths. Short effective fracture length, relative to created fracture length, has been linked to fracture fluid properties and their interaction with the formation (Bennion, 1996).

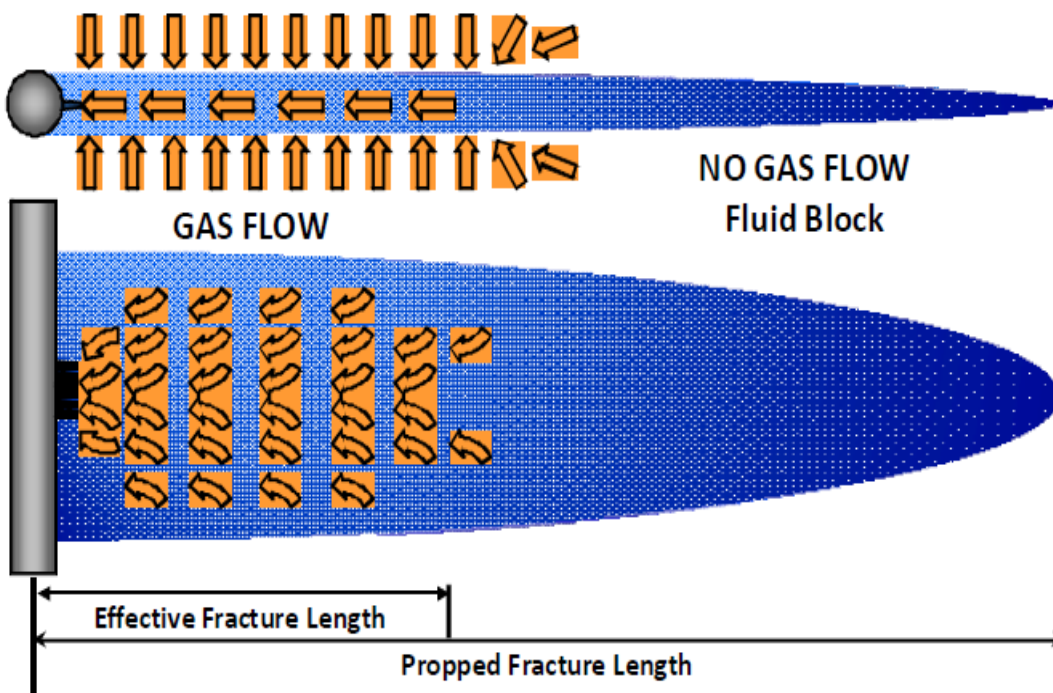


Fig 2.2 (Tudor, Nevison, and Allen 2009).

Interaction of the fracture fluid with the formation may result in a less than desired clean up, short effective fracture length and poor production. These issues have been described as resulting from water imbibition, phase trapping, sub-normally saturated reservoirs, and under-pressure reservoirs (Bennion, 1996). While the results of short

effective fracture lengths have been recognized in bi-wing fracture theory, non-contributing factors are still unresolved in created fracture volume theory, (Tudor, Nevison, and Allen 2009).

While the effective fracture length is affected by such factors as non-Darcy flow, it is related directly to fracture cleanup, and increases with time. From this study we found that the rate of fracture fluid production is affected significantly by the conductivity of the fracture. Greater dimensionless fracture conductivity results in more effective well cleanup, longer effective fracture lengths versus time, and greater effective stimulation of the well (Lolon, McVay and Schubarth, 2003).

$$(2-1) \quad C_R = \frac{W * k_f}{\pi * K_f * L_f}$$

$$F_{CD} = \frac{W * k_f}{\pi * K * L_f}$$

CR: dimensionless fracture conductivity

F_{CD}: dimensionless fracture conductivity

L_f: fracture half-length, ft

W*k_f: fracture conductivity, md-ft

K: formation permeability, md

K_f: fracture permeability, md

Constant

= 3.1416 π

Lolon, McVay and Schubarth (2003) results state that: Greater dimensionless fracture conductivity results in longer effective fracture lengths and greater cumulative gas production. This is because fracture fluid recovery increases with increasing fracture conductivity. The fracture cleans up faster with higher gas flow rates. However, the effective fracture length is still affected more by fracture conductivity than by gas flow rate. The effective fracture length is affected more by fracture conductivity than by formation permeability, fracture closure effects, and reservoir water mobility. Stabilized pressure gradients in the fracture is affected more by the conductivity of the fracture than by multiphase and non-Darcy flow effects. Effective fracture

lengths and fracture conductivities calculated from Pressure Transient Analysis (PTA) are significantly lower than the actual values due to multiphase and non-Darcy flow effects. At early times, the fracture lengths from PTA are low due primarily to cleanup effects, while non-Darcy flow and multiphase effects influence the calculated fracture lengths from PTA at late times.

Recently conducted a study that showed the effects of non-Darcy flow on pressure transient analysis of hydraulically fractured gas wells. This study revealed that calculated fracture half-lengths and fracture conductivities can be reduced by over 90% due to non-Darcy flow effects. These authors suggested that the best estimates of formation permeability, fracture half-length, and fracture conductivity can be obtained using a reservoir simulator that is capable of handling non-Darcy flow and fracture closure effects (Alvarez, et. al 2002).

AS Wei and Holditch (2009), to optimize a fracture treatment, the design engineer needs to consider both the costs of a fracture treatment and the effects of fracture half-length on the recovery of gas from the reservoir. There are a few well-known tendencies in fracture length creation that need to be discussed here to set the stage for our analyses. First, as the value of propped length increases, the cumulative gas production and revenue will also increase. However, as the fracture half-length increases, the incremental gas recovery benefit decreases in terms of $\Delta G_p / \Delta L_p$. The incremented gas production, ΔG_p , per foot of incremental propped fracture length, ΔL_p , is a monotonically decreasing function.

Second, as the volume of fracture treatment increases, fracture half-length also increases, provided the fracture height is not growing unconfined. As the fracture length increases, the incremental cost of each foot of fracture also increases. Because the fracture width is also increasing, the ratio of $\Delta V_{ft} / \Delta L_c$ is an increasing function. In other words, to create additional created fracture length, ΔL_c , larger volumes of fracture fluid, ΔV_{ft} , are required.

Wei and Holditch are calculated the incremental cost of the treatment is compared to the incremental benefit of increasing the treatment volume, an optimum propped fracture length can be found so to calculate the optimum fracture half length, we need do the following steps.

- Using appropriate reservoir data, we need to determine the layers of rock that will be fracture treated in a given fracture treatment stage.

- Once the reservoir properties have been defined, we need to select a fracture fluid and a propping agent for the treatment design.
- To run the simple fracture design models, we need to determine a pumping schedule.
- With a known pumping schedule, a maximum fluid volume and proppant mass can be estimated. We can estimate the created and propped fracture half-length for a fixed value of fracture height and various fluid and proppant volumes.
- For given values of propped fracture half length, we can estimate gas production for fixed values of time, such as 5 years or 10 years.
- Using data from the design and cost estimates from the service companies, we can estimate the costs to create certain values of propped fracture length.
- Comparing revenue versus cost, we can estimate values of optimal fracture length.

Holditch and Bogatchev (2008) simple rule of thumb looks at optimal fracture length as a function of drainage area for given estimates of formation permeability.

$$X_f = C * \ln(A) + d \quad (2-2)$$

Where:

- X_f = optimal fracture half-length, ft

- k = formation permeability, md

- c, d are the correlation coefficients.

- $c = -0.1818 \cdot A - 24.6220$

- $d = 231.23 \cdot \ln(A) - 615.37$

- A = drainage area, acres

It is determined that the performance of a hydraulically Fractured vertical well with mechanical skin and fracture half-length can be substituted by the performance of a fractured half-length with no skin. A hydraulic fracturing treatment should be designed based on reservoir properties, the economics of the well, well spacing desired propped fracture length and desired productivity index increase (which depends on the areal extent of the fracture). In addition to mechanical properties of the rock, proppants

Concentration%. Viscosity and injection rate of the fracturing fluid the leak off of the fracturing fluid into the formation is also an important factor affecting the volume (or size) of the induced hydraulic fracture. Hydraulic fracturing models that predicts the width length and height of the created fracture had been developed that takes into account the above mentioned parameters (Malekzadeh, Farid and John 1995). Malekzadeh, Farid and John (1995) results obtained using the new model indicates that a small change in mechanical skin (i.e., S) factor based on its conventional definition has a significant effect on the fraction of the hydraulic fracture length contributing to unrestricted production. As the fracture penetration ratio and (X_e/Y_e) ratio increase, hydraulic fracture productivity increases. Also at low fracture penetration ratio, a hydraulic fracture is more effective in a square drainage area than in a rectangular drainage area. (X_e, Y_e) =Rectangular reservoir dimensions, ft.

Holditch. (1978) investigated the effects of well spacing and fracture length on well productivity in low permeability gas reservoirs studied three examples that represented high, low and medium permeability gas reservoirs. They concluded that the most important parameters determining the optimum fracture length are the formation permeability and the initial gas in place. For high permeability reservoirs, they found that short fractures and large well spacing provide the optimum profit, whereas for tight gas reservoirs, long hydraulic fractures and small well spacing are required to optimize profit from the reservoir.

Narayanaswamy et al. (1998) the condensate saturation and gas relative permeability near the wellbore are a strong function of the trapping number. They also found that the effects of condensate dropout on gas relative permeability are closely coupled with non-Darcy effects that can be significant in high rate wells. Also they have shown that reservoir heterogeneity plays an important role in determining the effective of (non-Darcy flow coefficient) for gas inflow into high rate gas wells.

Indriati. (2002) proposed a model to predict the performance of hydraulically fractured gas condensate reservoirs, and calculate optimum fracture length. Their work showed that condensation accumulation causes the optimum fracture length to be larger than the zero-fracture-face-skin optimum. For every flowing bottom hole pressure, they found that there exists an optimum fracture geometry that maximizes the dimensionless productivity index.

Aggour. (1998) did economic optimization studies combining high-permeability fracture modeling with expected well. Performance and NPV calculations. They found that in high-permeability reservoirs, fracture conductivity is more critical than fracture length. They also found that larger drainage areas would require larger designed fractures to achieve maximum economic returns.

Peaceman.(1983) was used to calculate the equivalent well radius.

$$(2-4) \quad r_e = 0.28 \frac{\sqrt{\Delta X^2 * k_y + \Delta Y^2 * k_x}}{\sqrt{k_y} + \sqrt{k_x}}$$

Mohan *et al.* (2006) the Optimum Fracture Length Analytical Model for Darcy Flow, above the Dew Point an analytical expression for the optimum fracture half-length for flow above the dew point without non-Darcy effects has been derived in

The final equation obtained is:

$$(2-5) \quad L_{opt} = \sqrt{\frac{V_p K_f}{2\pi K h (1 - \phi_f)}}$$

V_p = proppant volume

k_f = fracture permeability

h = formation thickness

ϕ_f = fracture porosity

k = reservoir permeability

It is clear from the above expression that the optimum fracture length is smaller for thick, high permeability reservoirs and increases with the fracture conductivity and proppant volume.

The Optimum Fracture Length Analytical Model for Darcy Flow below the Dew Point Below the dew point, a condensate bank builds up around the fracture. An analytical expression for the optimum fracture half-length for flow below the dew point has been derived in Appendix A and is given by:

$$L_{opt} = \frac{-kr_d(1 - k_{rg}) + \sqrt{\pi \frac{V_p}{2h(1 - \phi_f)} k k_f}}{\pi k - \frac{kr_d(1 - k_{rg})^2 2h(1 - \phi_f)}{V_p k_f}} \quad (2-6)$$

The above equation shows the effect of the gas relative permeability and the depth of the condensate bank on the optimum fracture length

For flow above the dew point, the above expression reduces to:

$$L_{opt} = \frac{\left(\frac{V_p}{2\pi h(1 - \phi)} \right) + \sqrt{\left(\frac{V_p}{2\pi h(1 - \phi)} \right)^2 + \frac{8\mu h r_w}{k\rho\beta_1 q} \left(\frac{V_p}{2\pi h(1 - \phi)} \right)^2}}{2r_w} \quad (2-7)$$

Optimum Fracture Length: Analytical Model with Non-Darcy Flow in the Fracture an analytical expression for the fracture half-length for flow below the dew point with non-Darcy effects in the fracture has been derived in Appendix A and is given by:

$$L_{opt} = \frac{\left(\frac{V_p}{2\pi h(1 - \phi)} + \frac{k_{rg} * r_d * r_w}{\pi} \right) + \sqrt{\left(\frac{V_p}{2\pi h(1 - \phi)} + \frac{k_{rg} * r_d * r_w}{\pi} \right)^2 + \frac{8\mu h r_w}{k\rho\beta_1 q} \left(\frac{V_p}{2\pi h(1 - \phi)} \right)^2}}{2r_w} \quad (2-8)$$

To simplified expression neglecting non-Darcy flow can be obtained from the analysis by putting $\beta_1 = 0$ Mohan (2006b) study Reservoir Properties for single-layer reservoir was used for this study. The reservoir is homogeneous with a uniform porosity of 20% and a uniform permeability of 1 mD. It has a net-to-gross ratio of 0.5. The reservoir dimensions are 5000 ft. x 5000 ft. x 57 ft. thick. The fracture permeability is 7000 mD. Mohan was use Initial Conditions for this reservoir pressure and temperature are 5900 psi and 275oF for the lean fluid and 3400 psi and 320oF for the rich fluid. Initial water and gas saturations are 0.3 and 0.7, respectively. Also use Well Model. The single well considered in this study is operating with a minimum bottom hole pressure constraint

of 1500 psi, which is below the dew point pressure. The well bore radius is 0.25 ft, plotting the cumulative gas produced at 1000 days against fracture length for a given volume of proppant injected, this maximum corresponds to the optimum fracture length for that particular proppant volume. This is illustrated in Figure (2.3) Dimensionless plots of optimum fracture half-length against proppant mass above and below dew point, respectively, are shown in Fig(2.4). The optimum fracture length for a fracture permeability of 7000 md is greater than that for a fracture permeability of 1000 md.

Bilu Cherian *et al.* (2009) observed that the key to the success of a tight-gas field development program in a fluvial environment is to understand the reservoir's deliverability and what the optimum fracture half-length is as a function of geological setting and stress state. He was numerous completion strategies (Limited Entry, high rate limited entry, and various Pin-point Stimulation Techniques) were implemented with an appropriate data collection strategy to evaluate and compare well performance. Micro seismic data, tracer logs, and pump-in data were used to calibrate and constrain appropriate fracture evaluation models (P3D and 3D). Rate-transient production analysis techniques, together with statistical data techniques were incorporated to evaluate stimulation techniques (proppant & fluid volumes) and to validate the differences/ similarities observed between micro seismic and fracture-propagation model predicted lengths.

Poe and Conger (2009) a single well rate-transient based analysis for fractured wells together with production rate and production pressure history match was utilized. This technique can be used to obtain quantitative estimates of the reservoir effective permeability effective fracture half-length, and average fracture conductivity (provided certain flow regimes or limits of the flow regimes are exhibited in the production data) together with production history match.

Cherian *et al.* (2009) they observed that In Fig(2.5) shows the agreement with the fracture pressure history match half-lengths and the productive half-lengths calculated from Production history matching and rate-transient analysis. The productive half-lengths and propped half-length in the first four cases differed significantly possibly due to the impact of effective stresses on propped lengths. Where significantly lower than micro-seismic lengths, but were within (60-75) % of the

propped lengths calculated from fracture pressure history matching. This corresponds to about 42 percent of micro-seismic lengths. Also observed that Casing pressures was increased by 1,200- 2,500 psi on implementation of the design changes (sample size: 20 wells) and production logs confirmed observation of a significant increase in bottom hole producing pressures (1,500 psi). When fracture pressure history match was performed on these well to quantify the difference analysis indicated that propped fracture half-lengths were significantly larger when injection rates were significantly higher (1.5 times greater than conventional designs)

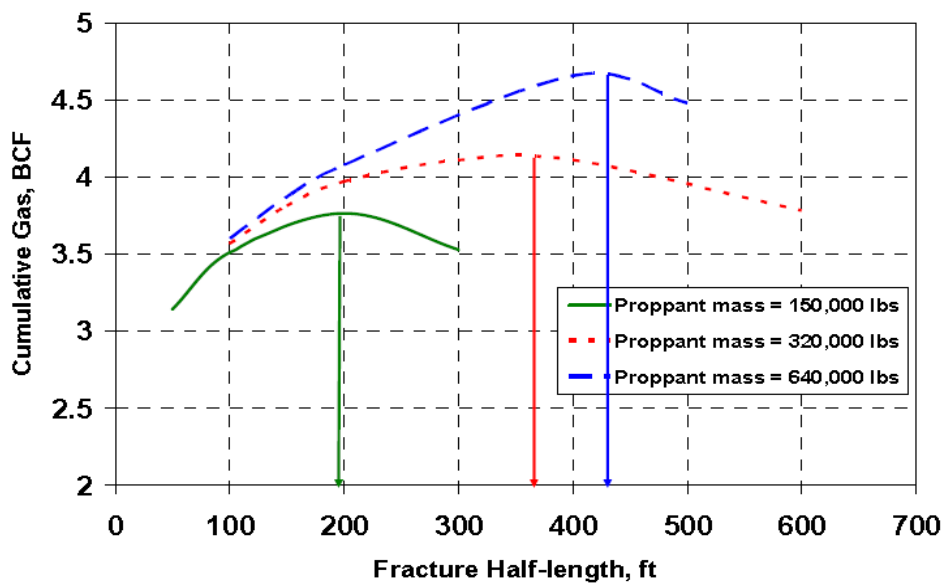


Fig 2.3 Mohan. (2006).

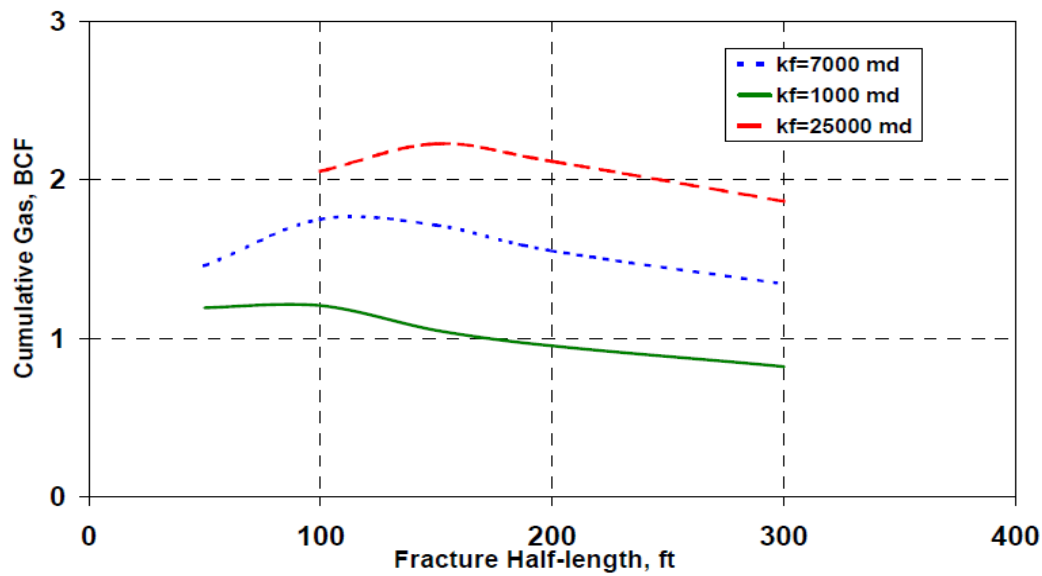


Fig 2.4 Mohan. (2006)

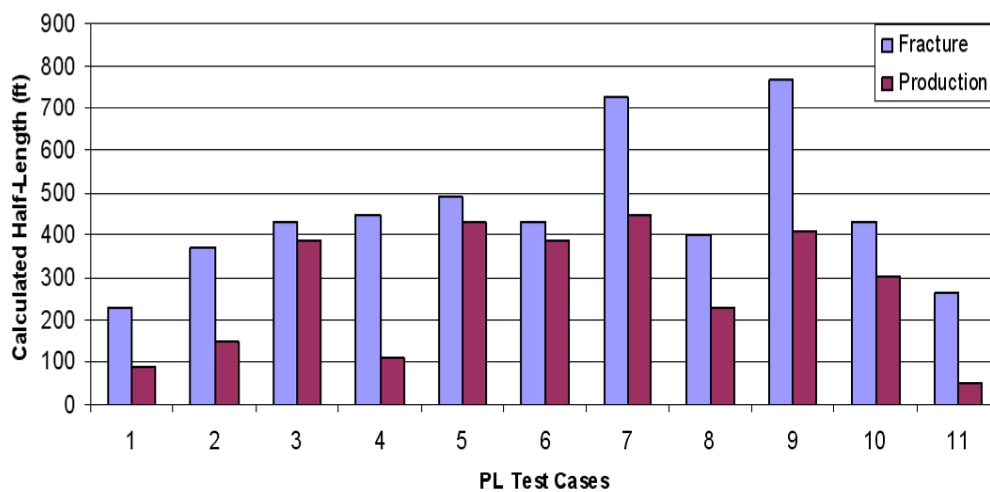


Fig 2.5 Cherian et al. (2009)

Preliminary evaluation of fracture pressure history match length vs. length calculated from production analysis. Lough *et al.* (1997, 1998) developed a numerical method to compute the effective permeability of simulation grid-blocks with realistic fracture characterizations. Although this method handles generalized fracture

geometries, it is numerically inefficient for the case where many small fractures exist.

The method can also underestimate the flow contribution from long fractures. Lee *et al.* (1999) developed a hierarchical approach to model flow in a naturally fractured reservoir with multiple length-scale fractures. Kamath *et al.* (1998) showed that disconnected fractures cannot be ignored as they can significantly contribute to the overall flow through the rock matrix. They also showed that the effective permeability is much larger than a simple sum of fracture and matrix permeability's, as is commonly assumed. Barree *et al.* (2006) used different methods: fracture modeling, PDA, and PTA techniques to determine the fracture length. They noted the discrepancy in the analysis results and concluded that non-Darcy flow, multiphase flow, proppant conductivity damage, and model applicability could lead to the effective fracture lengths being less than the designed fracture lengths.

Crafton and Anderson (2006) used a method called Reciprocal Productivity Index (RPI) to evaluate early time production data. Their study shows that the computed effective fracture lengths are quite shorter than the design lengths. Barree *et al.* (2003) reported that the effective or "cleaned up" fracture length is a function of dimensionless fracture conductivity ($F_{CD} = k_f * w_f / X_f * k$) and the critical dimensionless fracture conductivity (F_{CDcrit}) required to cleanup fracture fluids. The apparent producing fracture half-length, including the effect of gel plugging, is calculated from the effective infinite conductivity fracture half-length given by first equation and the final apparent producing half-length, given by second equation

$$\frac{X_{eff}}{X_{created}} =$$

$$(2-9) \frac{1}{1 + \left(\frac{F_{cd}}{1.7}\right)^{-1.01}}$$

$$X_{app} =$$

$$(2-10) \frac{X_{eff}}{1 + \left(\frac{30}{1.7 F_{cdcrit}}\right)^{-1.01}}$$

Smith *et al.* (2004) studied the effects of non-Darcy flow on fracture conductivity and effective fracture length. The potential reasons for the shorter than desired effective fracture lengths were identified, with the most likely being reservoir heterogeneity, excessive fracture height growth and poor fracture fluid cleanup.

Elbel and Ayoub (1992) noted that design shortcomings due to inappropriate fracture geometry and design parameters as well as well test analysis shortcomings are the main causes for an apparent shorter fracture length than designed. Rushing and Blasingame (2003) observed good agreement with effective fracture half-lengths computed from Production data analysis (PDA) and pressure transient analysis (PTA) methods .

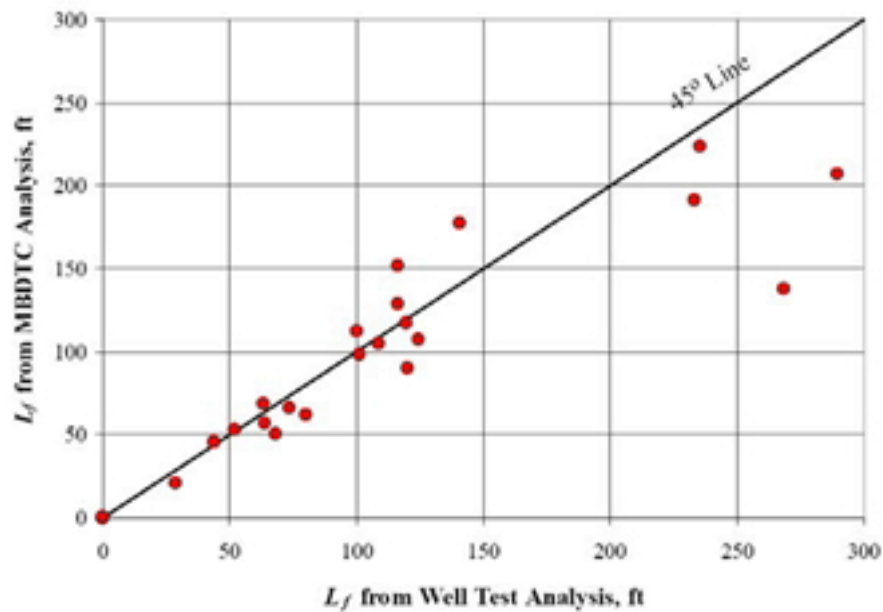


Fig 2.6 Rushing and Blasingame (2003)

Lee and Holditch (1981) presented the results of well test analysis (PTA) and numerical simulation history matching from 13 hydraulically fractured, gas wells. The results show that the numerical simulation (history-match) fracture lengths averaged about 68% of the design lengths and the fracture lengths calculated using the modified linear flow technique (PTA) averaged about 79% of the design lengths.

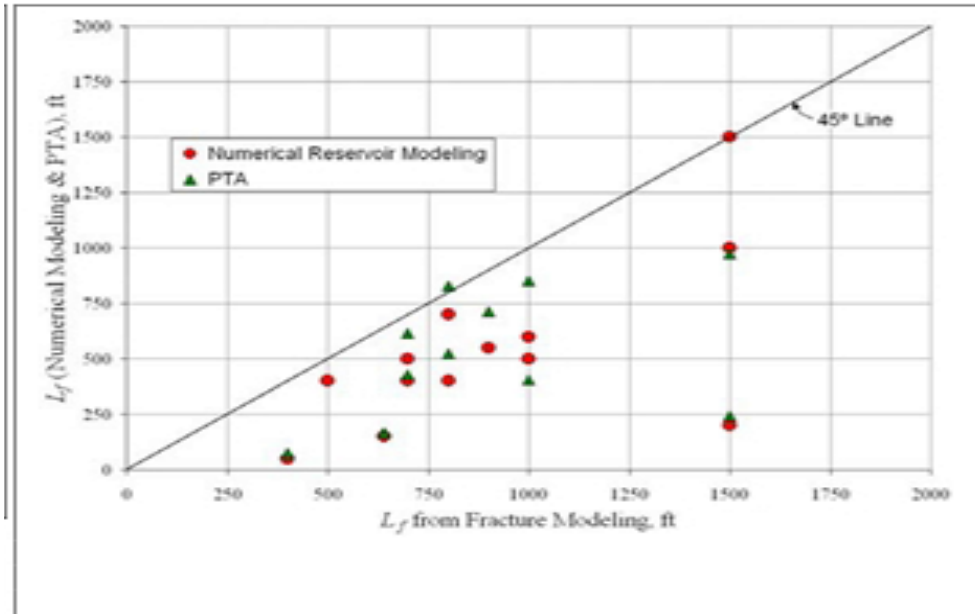


Fig 2.7 Lee and Holditch (1981).

Cipolla *et al* (2008). Reported that the Production analyses and reservoir simulation history matching can result in non-unique interpretations of effective fracture length and conductivity in the absence of accurate measurements of reservoir permeability and pressure. Also Micro seismic and/or tilt fracture mapping can provide direct measurements of created fracture length and fracture complexity, but cannot provide insights into the propped and effective fracture length.

R.D. Barree *et al* (2003), stated that “effective” fracture half-length is much lower than the designed half-length, due to poor fracture-height containment, poor proppant transport, proppant falling out of zone (convection), ineffective proppant-pack cleanup, capillary-phase trapping, multiphase flow, gravitational-phase segregation, and non-Darcy flow.

They presented detailed evaluations of hydraulically fractured well behavior using Gas Production Analysis & Pressure Transient Build Up, on two wells produce from sandstone formations, the pressure-transient tests are of sufficient quality to estimate fracture half-length. The fracture half-lengths predicted by the PBU analyses are much longer than those given by GPA. An apparent discrepancy remains between the created fracture half-length of more than 1,000 ft (as predicted by the fracture-treatment history match) the PBU length of 400 to 600 ft, and the effective length of less than 30 ft for both wells.

The various damage mechanisms they accounted include: loss of pack width and permeability caused by closure stress on the proppant pack. The effects of pack compression are shown as pack permeability and external-pack width. The internal-pack width results from additional width losses caused by dynamically deposited filter-cake residue and formation spilling into the proppant pack. The amount of filter cake depends on the polymer-gel loading, type of polymer and breaker, fluid efficiency, fracture geometry, and producing-flow rate. High flow rates tend to abrade and erode the filter cake. The non-Darcy loss given in the table is defined by

$$F_{nd} = \left(1 + \frac{\beta k_f \rho v}{\mu}\right) \quad (2-11)$$

F_{nd} = non-Darcy conductivity multiplier

k_f = effective permeability to gas in the fracture, md

ρ = density, g/cm³

μ = viscosity, cp

v = superficial fluid velocity cm/s

β = Forchheim initial coefficient

The Regained-permeability factor quantifies the permeability loss caused by gel residue dispersed throughout the pack. The Infinite conductivity half-length gives the effective fracture length after accounting for these damage factors.

The effect of gel-pseudo yield point is accounted for by use of an empirical relation to a characteristically critical incremental dimensionless fracture conductivity (F_{CD}) for fracture cleanup. The x_f at F_{CD} represents the final apparent fracture length under flowing conditions.

$$X_{fa} = \frac{X_{fa}}{1 + \left(\frac{F_{CD}}{1.7}\right)^{-1.01}} \quad (2-12)$$

The most significant losses to conductivity are caused by non-Darcy flow, filter cake, and gel residue (regained permeability). If the dynamic conductivity losses are assumed to approach zero after shut-in, the effective fracture length and conductivity can be estimated from

$$F_{CD} = \frac{K_f W_f}{K_f X_{df}} \quad (2-13)$$

$$X_{fa} = \frac{X_{fd}}{1 + \left(\frac{F_{cd}}{1.7}\right)^{-1.01}} \quad (2-14)$$

W_f =fracture width

X_{df} =designed fracture half length

X_{fa} =apparent fracture half length

The value of X_{fd} is the designed or created half-length and k_{fwf} represents the proppant-pack conductivity (static damage only). The effective producing length, as shown by GPA production analysis, is much shorter than the apparent PBU length. The difference is attributed to dynamic-flow effects associated with multiphase and non-Darcy flow.

Agarwal *et al.* (1999) and Gardner *et al.* (2000) estimated the effective drainage area. This technique uses a plot of reciprocal dimensionless-wellbore pressure, $1/p_{wD}$ vs dimensionless- cumulative production, Q_{DA} , to generate the rate-cumulative-decline curve.

$$Q_{DA} = \frac{tDA}{P_{wD}} = \frac{4.5TziGi \Delta m(\bar{p})}{\phi h A p_i \Delta m(\bar{p})} \quad (2-15)$$

$$P_{wD} = \frac{Kh \Delta m(p)}{1422Tq(t)} \quad (2-16)$$

$$t_{DA} = \frac{0.006328Kta}{\phi(\mu Ct) i A} \quad (2-17)$$

Q_{DA} = dimensionless cumulative production based on area (A)

P_{wD} = dimensionless wellbore pressure

t_a = pseudo equivalent time, days

t_{DA} = dimensionless time based on area (A)

Once the effective drainage area has been determined, the reservoir-flow capacity, or transmissibility, and effective fracture half-length can be derived from a semi log plot of normalized pressure vs. adjusted time and from type-curve matching. Elbel and Ayoub (1992), discussed the possible reasons for why well test analysis often indicates short fracture lengths even after large volumes of fluid and proppant

have been injected into the formation. The calculated fracture length will be off by a factor equal to the dimensionless layer conductivity C_{TD} which they defined as:

$$C_{TD} = \sum \sqrt{\frac{(K\phi Cth^2)*l}{K\phi Cth^2}} \quad (2-18)$$

C_{TD} =Dimensionless Fracture Conductivity

ϕ = porosity, fraction

Ct = total compressibility

The C_D is dependent on the ratios of the parameters, these ratios can be determined from core measurements or log analysis. We use C_{TD} when there is no vertical communication between layers, and during transient behavior.

Camacho A. *et al.* (1987) showed that the apparent fracture length, L_u (in) such cases will be:

$$L_{xa} = \sum CtD * Lxf \quad (2-19)$$

L_{xa} =apparent fracture half-length, m

L_{xf} =fracture half-length, m

Meehan, Horne and K. Aziz (1988) presented a solution for uniform flux fractures which accounts for fracture azimuth. Knowledge of the fracture azimuth will optimize the number of wells, the placement of the wells, and the length of the fractures. Numerical simulation of high conductivity fractures confirms that knowledge of fracture azimuth will be important for cases for which the ratio of interwell distance to fracture length is less than 2.0. They argued that as fracture length grew large compared to the interwell distance, the effect of fracture azimuth increased.

Holditch *et al.* (1978) combined a fracture simulation program with a simple type curve model and linked the two with an economics model.

Holditch concluded that formation permeability and gas-in-place per acre were the most significant factors relating to determination of optimum fracture length, and that longer fractures and shorter well spacing's were dictated by decreasing permeability's. Their model completely neglects fracture azimuth.

When he built a computer model call STIMEX, Xiong *et al.* (1993) developed rules to determine the pumping schedule for a fracture treatment. The main input data for the rules were

The value of reservoir permeability and the fracture fluid viscosity. For example, for low permeability reservoirs, we need more slurry fluid stages so we could ramp up the proppant concentration slowly while pumping the treatment. For high viscosity fracture fluids, we can go to higher proppant concentrations for any given treatment. With the recommended pumping schedule and once the total fracture fluid volume is determined, we can calculate the mass of proppant, pad volume, and the fluid pumping volumes for all the proppant stages. Then, by using the PKN or GDK fracture propagation model and an estimated value of created fracture height, we can determine the correlation between fracture fluid volumes pumped and fracture half length (Wei and Holditch 2009).

For our work, the costs of a fracture treatment has been divided into the Fluid Costs, Proppant Costs, Work Over Costs, Pumping Charges and Fixed Costs for equipment, people and any other treatment cost that is not volume dependent. The fluid costs and proppant costs are correlated with fracture half length. With increasing fracture half length, the amount of proppant and fracture fluid required will increase. Therefore, the costs to generate the increasing fracture half-length will also increase. For a specific fracture half length, we can use either the PKN or GDK fracture model, along with a known pumping schedule, to determine the proppant mass and fracture fluid volume required to achieve a specified length. Then with known proppant prices and fracture fluid prices, the proppant costs and fracture fluid costs can be calculated. Because all the other costs are independent of fracture half-length and they are known values, we can easily develop a correlation between the total costs and fracture half length (Wei and Holditch 2009).

CHAPTER 3

METHODOLOGY

Chapter 3

Methodologies and Procedures

The current study analyze the effect of fracture length and fracture conductivity on well productivity for a gas well on block 8, through a numerical simulation study. Based on the available petro-physical information and the field geological model, with the target sands of Dindier II, a geological study and reservoir analysis was first conducted with Petrel simulation software by SUDAPET Company in Sudan. The

obtained static and dynamic models was converted to reservoir simulation software (Computer Modeling Group - CMG) to create different strategies for well production with the different fracture length and fracture conductivity. The following procedures are to analyze the daily gas and water flow rates and cumulative production under different values of fracture half-length and conductivity with IMEX (black oil) simulator:

1. The potential of primary production for desired well within 16 years without fracturing was first estimated
2. The effect of fracture length on the well under analysis with in this period was carried out.
3. Optimize the reasonable fracture conductivity that accord with the Reservoir characteristics.

Optimization of fracture length and conductivity in this study was based on the reservoir simulation only and did not include the Net Present Value (NPV) for this step, a reservoir simulator with refined grids near the well-bore is needed. Hence, Local Grid Refinement (LGR) was used to design the grid frame near the well-bore.

3.1. Global (Parent) Grid:

The Geological model used in this study was constructed by SUDAPET; to accurately describe the structure, a model of grid number $91 \times 128 \times 80$ with total cells of 931840 was conducted. The average cell sizes in X and Y directions are 24.25 ft with an average cell thicknesses (DZ) of 12.26 ft. Cartesian coordinate and corner point geometry was used to perform the analysis; the dry gas model simulation was started in 1, Nov, 2003 with one vertical well (Hossan -1) which completed with 7" production casing. Fig (3.1) presented a schematic diagram for formation and the layers (sub grid) which have been defined in the reservoir model.

3.2. Reservoir Rock and Fluid Properties

The Rock and Fluid Relative Permeability default table for shaly sand was used to generate the relative permeability curve as recommended by the original model creators as no SCAL data are available for the field.

The PVT were calculated by Petrel simulation program using Reference pressure of 2120.0 Psi and Reservoir temperature of 146°F. The minimum and the maximum pressure were 300.0 and 3865. 0 Psi respectively. The properties were calculated based

on the correlations presented through Table 3.1. The resulted PVT data for the gas were presented through Table 3.2

Table 3.1 PVT Correlation

Properties	Correlations
Z Factor	Hall & Yarborough (1973)
Gas Pseudo critical Properties	Piper, McCain & Corredor (1993)
Gas Viscosity	Lee, Gonzales & Eakin (1966).
Water Formation Volume Factor (P>Pb)	McCain (1990).
Water Compressibility (P>Pb)	Osif (1988) Valko & McCain (2003)
Water Viscosity	Meehan (1980).

The other control parameters of the formation and fluid are as follows:

Initial Conditions:

Reference pressure: 2119.7 psi

Reference depth: 4865.67 ft

Water gas contact: 4865.67 ft

Economic production limitation: **50000 SCF/d**,
Producers' minimum flowing pressure set to **200psi**,

Formation Water Properties

Water density @ surface: 63.69820224 lbm/ft³

Water formation volume factor: 1.00797121 RB/STB

Formation water's salinity: 30000 PPM

Formation water's viscosity: 0.47463036 cP

Compressibility of formation water: 0.00000276 1/Psi

Other information were presented in Table 3.3

Table 3.2 Gas PVT Properties

Pressure (psi)	Gas Formation Volume Factor (RB/MSCF)	Gas Viscosity (cP)
300	9.837633847	0.012483793
478.25	6.065695906	0.012743651
656.5	4.346019057	0.013049438
834.75	3.364350704	0.013398955
1013	2.731507669	0.013791572
1191.25	2.291262361	0.014227086
1369.5	1.968726098	0.014705151
1547.75	1.72349668	0.015224908
1726	1.531835328	0.015784734
1904.25	1.378853143	0.016382104
2082.5	1.254711755	0.017013573
2260.75	1.152624647	0.017674885
2439	1.067739372	0.018361185
2617.25	0.996481172	0.019067301
2795.5	0.936151531	0.019788044
2973.75	0.884673489	0.020518475
3152	0.840424237	0.021254107
3330.25	0.802121096	0.02199103
3508.5	0.768741141	0.022725961
3686.75	0.73946275	0.023456237

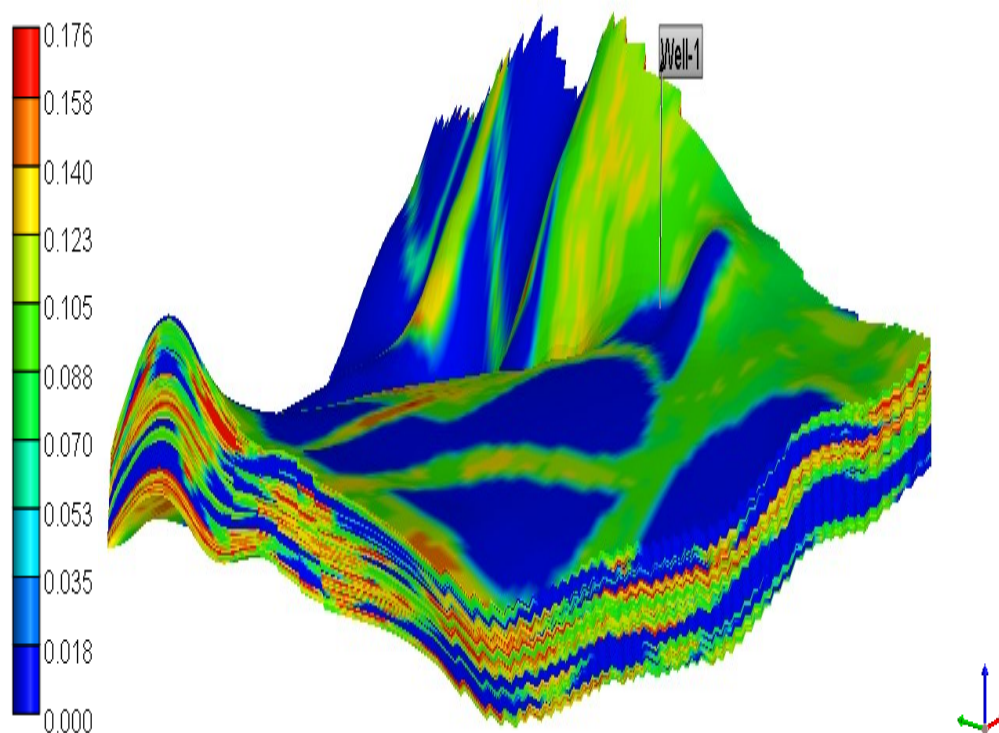


Fig 3.1 Schematic Diagram for Formation and Sub- layers for the Model

Table 3.3 is the available Well Test Results:

Property	Values
Wellbore storage, bbl/psi	0.0034
Permeability, md	46.1
Skin	26.5
Initial reservoir pressure at gauge depth, psi	2119.7
Productivity Index (PI), M scf/d/psi	25.282
Flow Efficiency (FE), %	20.04
AOF, MM scf/d	25.518

The primary objectives of Hosan-1 are the Dinder 3 sands and Lower Dinder 2 sands, and the secondary objectives are the Blue Nile sands, the Upper Dinder 2 sands and the shallow Dinder 1 sands which are oil bearing in Dinder-1 well. The well location selected is considered optimum to penetrate all the targeted zones with emphasis on the primary targets. In Dinder-1 well, overpressure was encountered from

Lower Dinder 3 sand downward. Similar overpressure zone may also exist in Hosan-1, which may assist in maintaining the porosity up to 25.6% at 3000m and 17% at 3625 m as seen in Dinder-1 well.

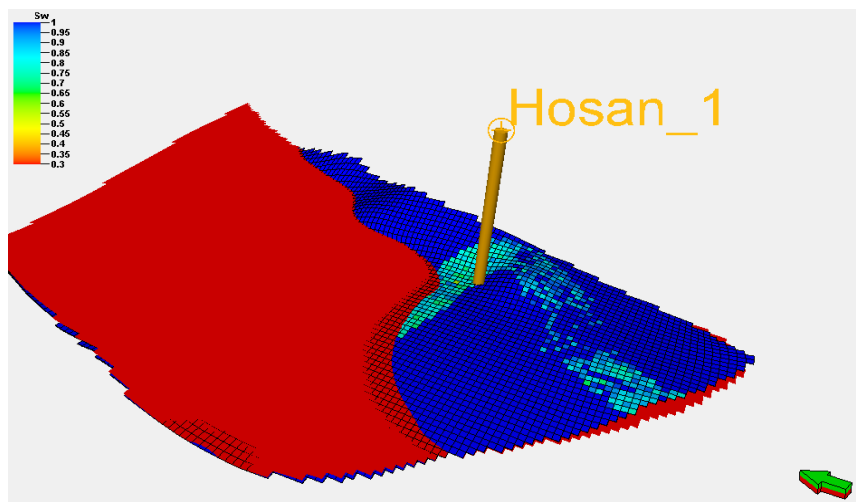


Fig 3.2 The Location of well Hosan -1

3.3. History Match

As histories match allowing making accurate predictions and evaluating alternative production scenarios; history matching was carried out manually, standard procedures were used to achieve a technically acceptable match. The target formation here is Dinder II which its original gas in place (GOIP) 5.2 MMM SCF and its initial oil saturation of 0.65; the well was put into production on Jan. 1, 2008, till Sep. 9, 2008 totally produce crude gas 1.1×10^6 scf.

The wells have gotten a good match, so the next accurate plan prediction can be designed by use of this history match. The history match plots of oil production rate, water cut, and BHP of the well are shown through Fig. 3.2 and Fig. 3.4. After a good history match was achieved; the simulation was run to predict the performance of the wells for 16 years.

The well is perforated to produce from Dinder II formation only at depth of 1510 to 1527 ft; the well has no open connection to Dinder I or Dinder III, the target of this study is Dinder II, however the perforation was changed to 1510 to 1520; the reason for that is there is mudstone barrier under it despite with the pretty good mudstone barrier above, also the distance between the bottom of pay zone and Gas water transition zone is 3 ft.

The simulation was run first to predict the performance of the well before fracturing. The model was started at 1/1/2016 using IMEX as simulator type and single porosity as porosity type. The saturation and the permeability distribution for the model at the beginning of the simulation was presented in Fig 3.5 and 3.6 respectively.

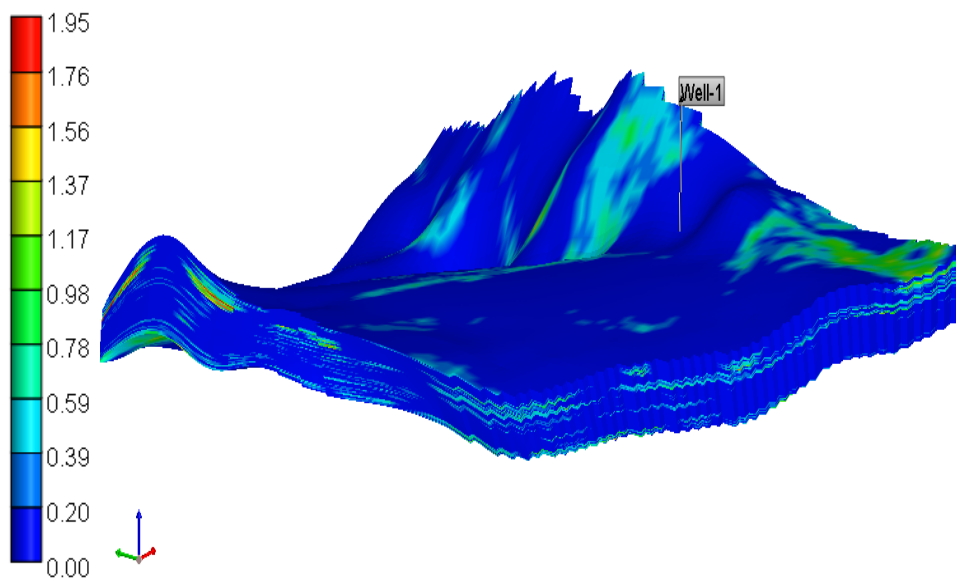


Fig 3.5 3D Viewer of Permeability Distribution at the Beginning of Simulation

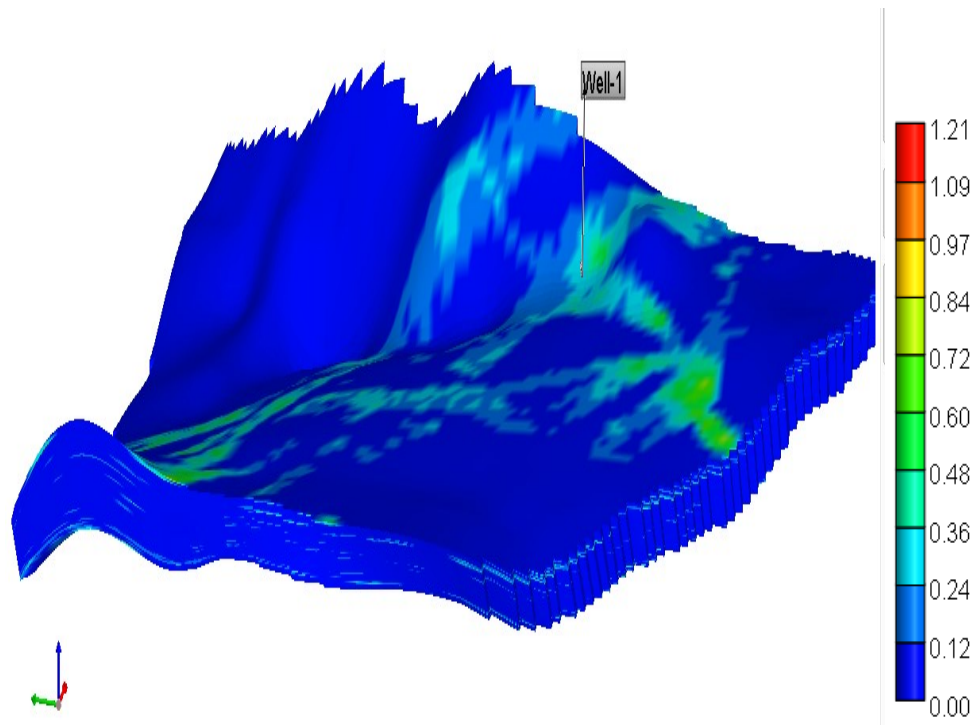


Fig 3.6 3D Viewer of Gas saturation Distribution at the Beginning of Simulation

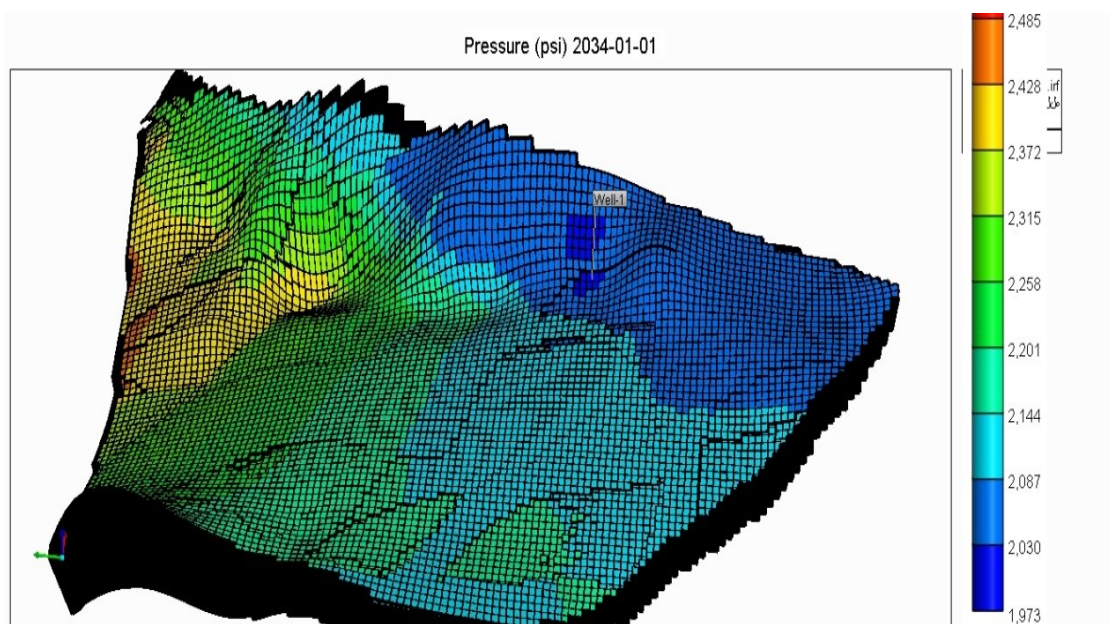


Fig 3.7 3D Viewer of Pressure Distribution at the Beginning of Simulation

3.4. Local Grid Refinement

Local Grid Refinement (LGR) is different-sized finite-difference grids: a coarse (parent) grid covering a large area which incorporates regional boundary conditions, and a fine (child) grid covering a smaller area of interest. Well Hossan-1 is located in the central of grids No. 51 in the X direction and grids No. 48 in the Y direction as presented in Fig 3.8. A fully three-dimensional, extremely finely grid is used to accurately model near well-bore and to perform fracture on the formation. The total number of the after LRG is 933073 increased by The grid contained the fracture is deal with a permeability of 80 to 100 times greater than the pay zone, while the other grid was kept on its global permeability. The width of the fracture was taken as 0.05 ft to allow the high proppant concentration to inter the fracture; the tested fracture length varying from 500 ft to 1200ft.

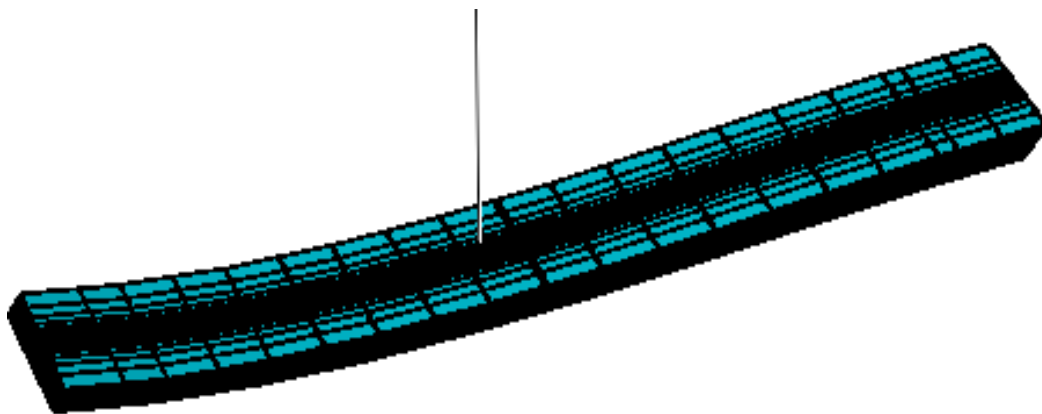


Fig. 3.8 3D Viewer showing Parent Grid and Child Grid of the LGR Model

3.5. Optimization of Fracture Length and Conductivity

The dimensionless fracture conductivity provides a means of optimizing the amount of fracture capacity for varying permeability and fracture length. Mathematically for pseudo-radial & pseudo- steady-state conditions, for a fixed volume of proppant, the optimum value for well productivity occurs at FCD value between 1 and 2.

For a given amount of proppant, two different types of fractures could be generated, a short fat fracture can be created with a high value of $k_f w$, or a longer, narrow fracture can be created with a lower value of $k_f w$.

Fracture parameters were optimized depending on the resulting gas production; when the increases of those parameters is not followed by considerable production to cover the cost of treatment and provides a considerable NPV, the increment is then unfavorable. According to the reservoir properties, the reservoir simulation software was run to study the effect of fracture length on gas production; the simulator was run using the reservoir model and the LGR presented through section 3.1 and 3.4 respectively.

First the **IMEX** simulator was run for the well without fracture to predict the well performance, then the fracture length ranging from 300-1000 ft, was used to study the effect of the fracture length; to study the effect of fracture conductivity on the gas production, the fracture length was kept constant for fracture conductivity of 1, 2, 3, 4, 5, and 100.

$$(3-1) FCD = \frac{k_f w}{k L_f}$$

Where

K_f = Fracture permeability (md).

W = Fracture width (ft).

L_f = Fracture half length (ft).

K_r = Reservoir permeability (md)

CHAPTER 4

RESULTS & DISCUSSION

Chapter 4

Results & Discussion

4.1 Optimum length selection

The model was run for six different scenarios, each one is a different fracture half length (Null, 300, 500, 700, 900 & 1000 ft). A dimensionless fracture conductivity (C_D), fracture width ($w=0.05$ ft) were fixed for all scenarios. Results were obtained as shown in figures below:

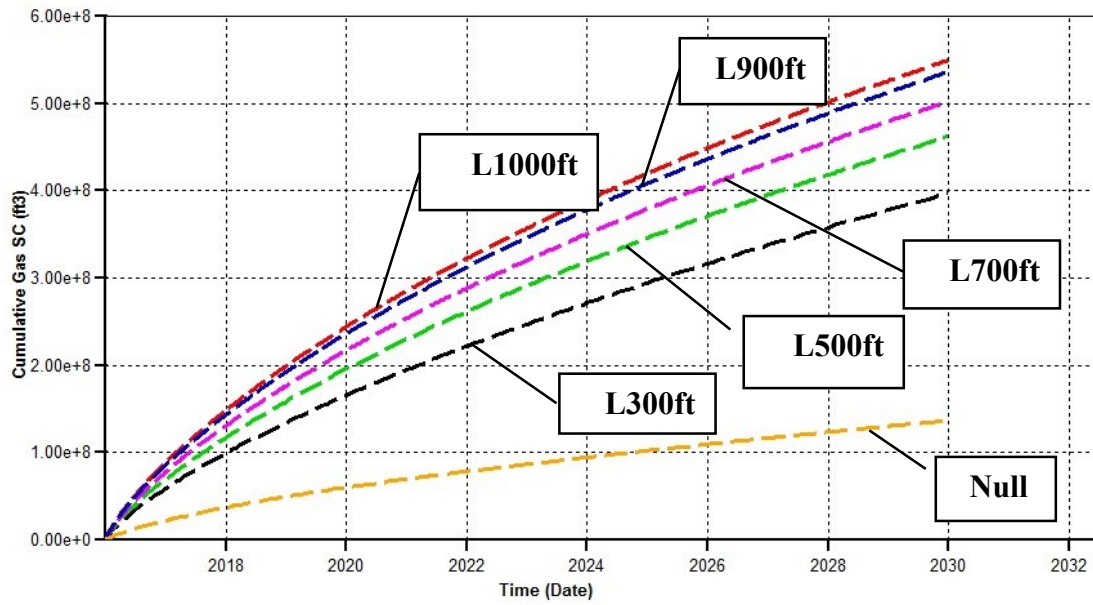


Fig 4.1: cumulative gas production for dimensionless conductivity 1 for different fracture lengths.

The first result shows the cumulative gas production for 14 years, the cumulative gas production without length is 136 MM ft³, increment in gas production 397MM ft³ could be seen if we create a 300 ft length fracture, and (462,502,537,550 MM ft³) for (500, 700, 900 and 1000 ft) respectively, Form the figuer above the increments in gas cumulative difference between curves (261,65,40,35 &13 MM ft³) will take place if we used as fracture lengths respectively except Null .

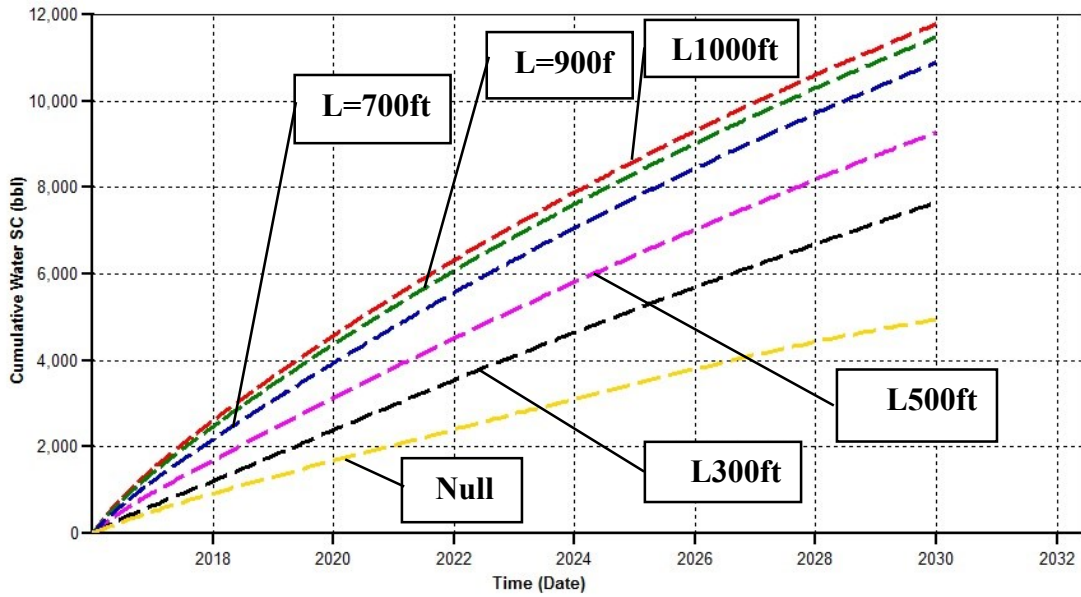


Fig 4.2: cumulative water production for dimensionless conductivity 1 for different fracture Length.

The first result shows the cumulative water production for 14 years, cumulative water production without fracture (4948 bbl) and (7660,9283,10905,11486 &11790 bbl) for (300,500, 700, 900 and 1000 ft) respectively, Form the figuer above the jumping in gas cumulative for each curve are (2712,1663,1622,581 &304MM ft³) will take place if we used as fracture lengths respectively except zero (ft).

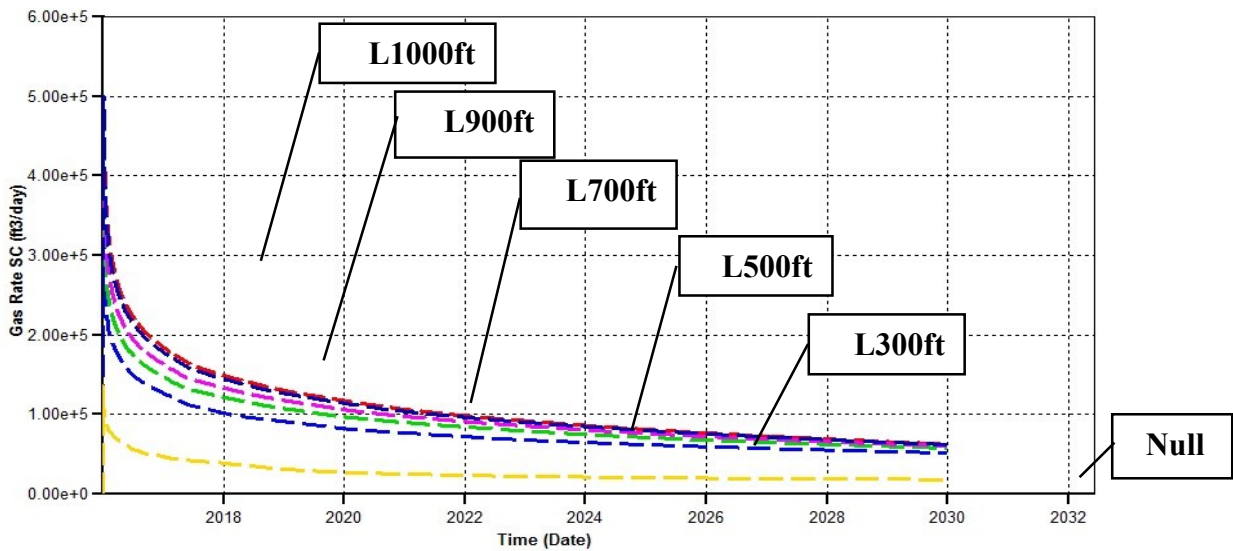


Fig 4.3: gas production rate for dimensionless conductivity 1 for different fracture lengths.

When it comes to gas production rate, from fig 4.3 a considerable incensement (364552 ft³/day) in gas rate will occur when create zero and 300 ft half-length fracture. The increment rate will be very low and almost insignificant as we move to the longer lengths, with almost the same rate at the final years of period.

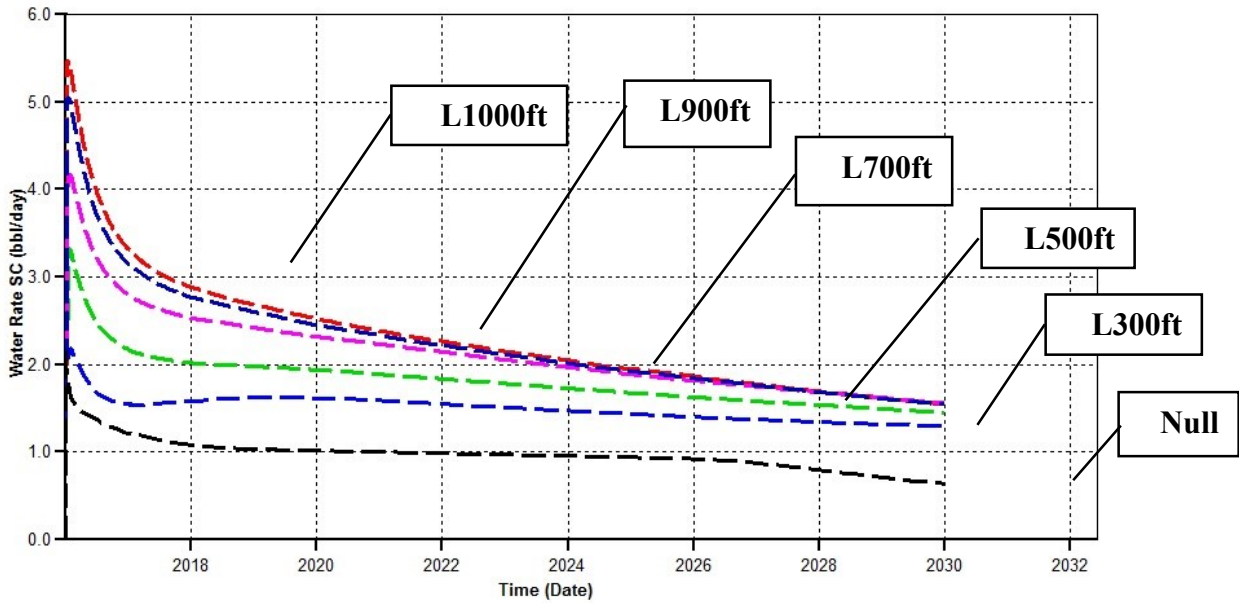


Figure 4.4: water production rate for dimensionless conductivity 1 for different fracture lengths

The water production rate from fig 4.4 in the early months, shows that an increment in water rater (1.7 bbl/day) will occur for 300 ft, and another greater increment (1.9 bbl/day) for 500 ft, and lesser increment if 700 ft length fracture is created. For length (700, 900 and 1000 ft) the increment is almost negligible. The water rate for the last years is semi identical.

Summary

Table 4.1 changing cumulative gas and water production according to difference lengths.

Length ft	Cumulative gas production MM cu ft	Cumulative water production bbl	Difference between gas cumulative MM cu ft	between water cumulative bbl Difference
0	136	4948	-	-
300	397	7660	261	2712
500	462	9283	65	1623
700	502	10905	40	1622
900	537	11486	35	581
1000	550	11790	13	304

From the Table optimum half-length based on gas & water cumulative when increase length from 700 to 900 ft the gas cumulative will be 537MM cu ft and the water cumulative 11486 bbl. The increment half-length to 900 ft the gas cumulative is 35 MM cu ft and the difference in water cumulative is 581 bbl.

So from previous result the optimum half-length is 900 ft.

4.2 Optimum conductivity selection

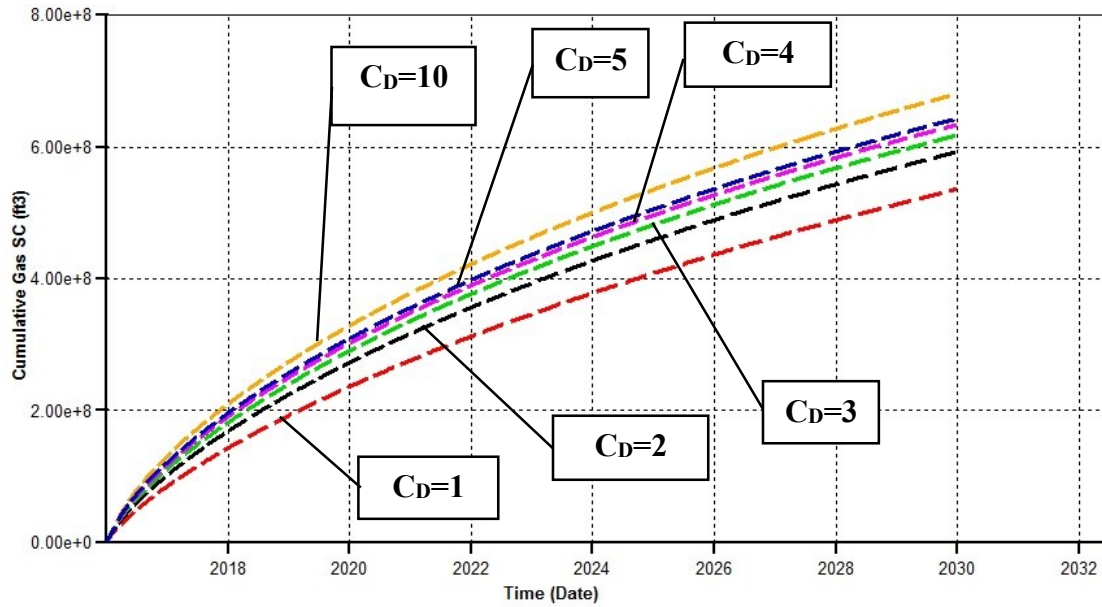


Figure 4.5: cumulative gas production for L=900 ft for difference dimensionless fracture conductivities (C_D).

The cumulative gass production during 14 years with dimensionless conductivities (1,2,3,4,5and 10) the increments in cumulativ gas production are (536,592,618,633,643and 681 MM cu ft) respectively.

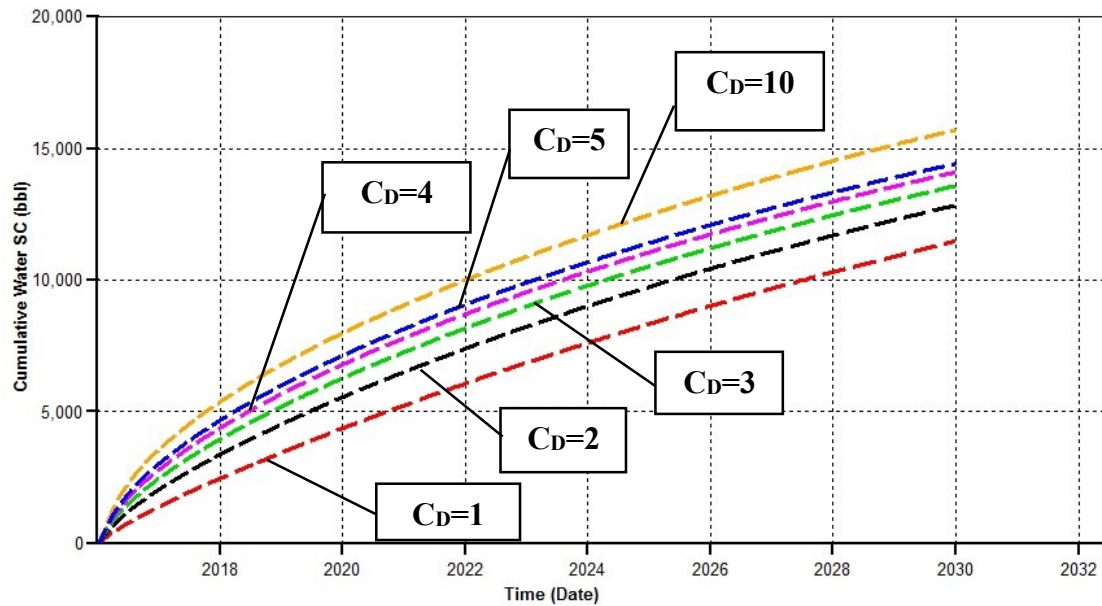


Figure 4.6: cumulative water production for L=900 ft for difference dimensionless fracture conductivities (C_D).

The cumulative water production during 14 years with dimensionless conductivities (1,2,3,4,5 and 10) the jumping in cumulative water production are (11486,12842,13585,14098,14419, and 15700 bbl) respectively.

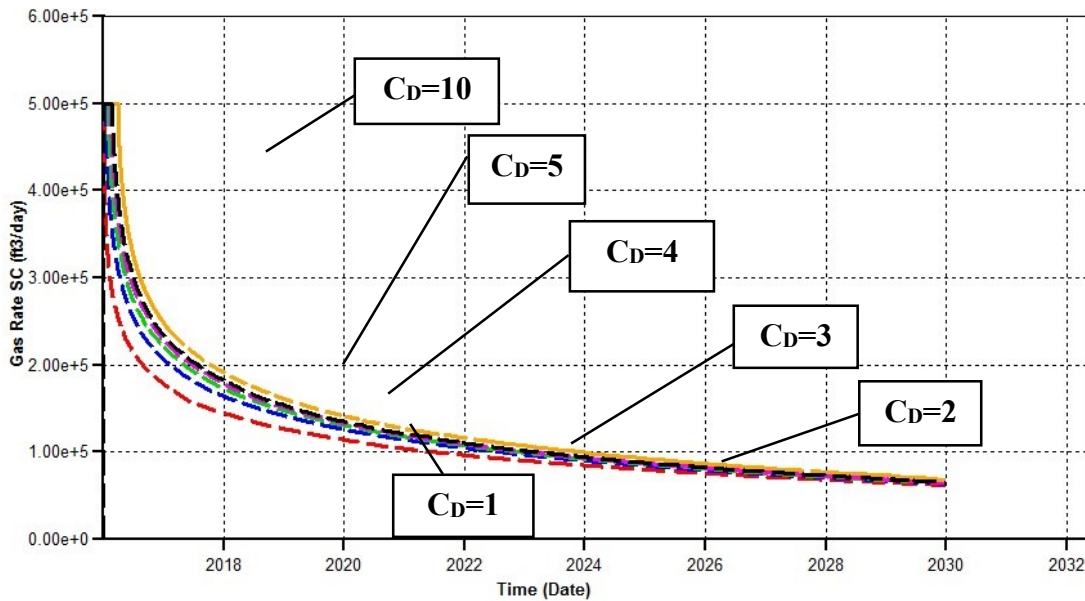


Fig 4.3: gas production rate for length 900 for different fracture dimensionless conductivity.

The gas production rate from fig in the early months, shows that all scenarios will reach a rate of 500000 bbl/day for all dimensionless conductivity, and the rate will start declining respectively.

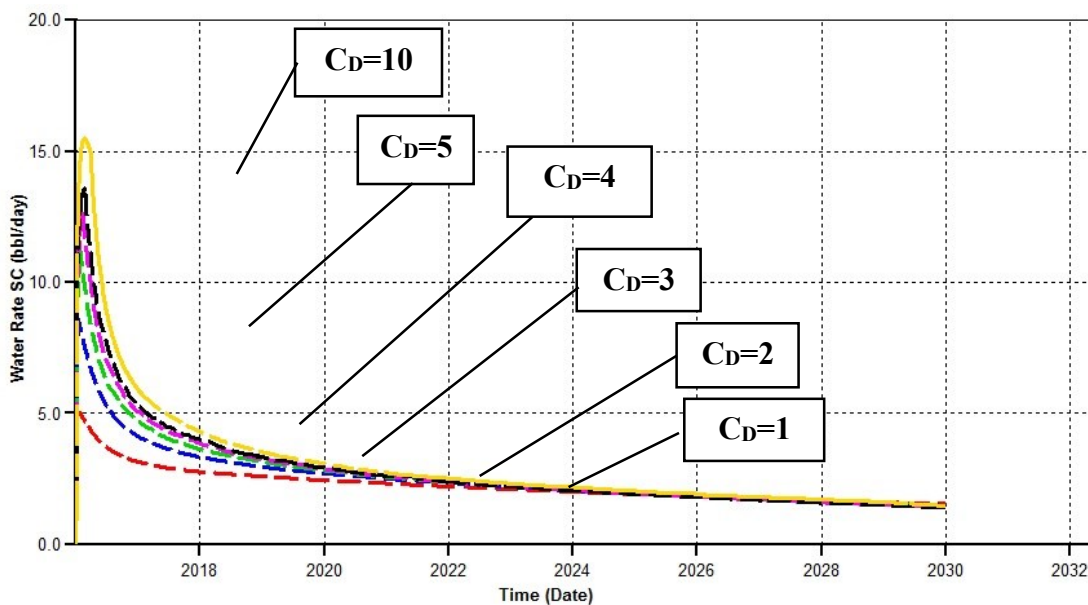


Fig 4.3: water production rate for half-length 900 ft for different fracture dimensionless conductivity.

The water production rate from fig 4.4 in the early months, shows that an increment in water rate (4.2, 7, 9.5, 11.4, 13, 16.6 bbl/day) for (300, 500, 700, 900, 1000 ft) fracture half-lengths. The water rates for the last years are almost the same.

Summary

Table 4.2 changing cumulative gas and water production according to difference Dimensionless conductivity.

Dimensionless conductivity	Cumulative gas production MM cu ft	Cumulative water production bbl	Difference between gas cumulative MM cu ft	Difference between water cumulative bbl
1	536	11486	-	-
2	592	12842	56	1356
3	618	13585	26	743
4	633	14098	15	513
5	643	14419	10	321
10	681	15700	38	1281

From the Table 4.2 optimum dimensionless conductivity - based on gas & water cumulative when increase dimensionless conductivity from 1 to 2 the difference between gas cumulative will be 56 MM cu ft and the water cumulative 1356 bbl, but the increment of dimensionless conductivity to 3 lead to difference between gas cumulative is 26 MM cu ft and the difference in water cumulative is 743 bbl. So the optimum dimensionless conductivity is 2.

CHAPTER 5

CONCLUSION & RECOMMENDATIONS

Chapter 5

Conclusion & Recommendations

5.1 Conclusion

Based on this study the following conclusions are made:

The study address the effect of fracture length and conductivity on well production in well Hosan-1 in Hosan field.

Fracture Length and fracture conductivity are strongly affect the fluid production at the early production time in this field.

A fracture length between 700 and 900 ft is the optimum length for the desired well to achieve good economic production fracture length grater small than this range can case either production restriction or unfavorable job. Fracture half-lengths selected to be **900** ft depends on the cumulative gas and water.

The best dimensionless fracture conductivity for the well was found to be **2**

5.2 Recommendations

- 1- Due to the limitation of data (2D seismic, no core, PVT and one well existing the uncertainty will be high.
- 2- The model summarized above is preliminary and subject to revision as additional data become available.
- 3- Based on the recommended fracture half-length and dimensionless conductivity, treatment cost including fluid and the best proppant type need to be performed.
- 4- Based on the recommended fracture half-length and dimensionless conductivity, future cost calculations and optimization based Net Present Value are required.

REFERENCES

References

- 1- Maimona Washie, Shale Gas Feasibility In Lacustrine Basin, Neem-Azraq Area, Muglad Basin, Sudan. North Africa Technical Conference and Exhibition, 20-22 February, Cairo, Egypt, 2012.
- 2- Elham Khair, Zhang Shicheng and Zhuang Zhaofeng, Primary Evaluation of the Sudanese Guar Gum with respect to the Hydraulic Fracturing Fluid International Journal of Scientific & Engineering Research, Volume 5, Issue 11, November-2014.
- 3- Elham Khair and Muhammad Faried, Preliminary Evaluation of Silica Sand in Sudan with Respect to Fracture Sand. J Pet Environ Biotechnol 7: 276. J Pet Environ Biotechnol 2016.
- 4- Agarwal, R.G. et al., 1999, "*Analyzing Well Production Data Using Combined-Type-Curve and Decline-Curve Analysis Concepts*", SPEREE (October 1999) 478.
- 5- Aggour T.M., and Economides, M.J..1998, "*Optimization of the Performance of High-Permeability Fractured Wells*", paper SPE39474, presented at the SPE International Symposium on Formation Damage Control, Lafayette, Louisiana, February 18-19.
- 6- Alvarez, C.H., Holditch, S.A. and McVay D.A.,2002,"*Effects of Non-Darcy Flow on Pressure Buildup Analysis of Hydraulically Fractured Gas Reservoirs*" ,paper SPE 77468 ,presented at the SPE Annual technical Conference and Exhibition, San Antonio, Texas, 29 September-2 October.
- 7- Barree R.D, Cox S.A, Barree, V.L, and Conway, M.W.,2003, "*Realistic Assessment of Proppant Pack Conductivity for Material Selection*", paper SPE 84306 presented at the SPE Annual Technical Conference and Exhibition, Denver, Colorado, 5-8 October.
- 8- Barree, R.D., Cox, S.A., Gilbert, J.V., and Dobson, M.,2003, "*Closing the Gap: Fracture Half Length from Design, Buildup, and Production Analysis*" ,paper SPE 84491, presented at the SPE Annual Technical Conference and Exhibition, Denver, Colorado, 5-8 October.
- 9- Bennion, D. B., Thomas, F.B., Bietz, R.F.,1996, "*Low Permeability Gas Reservoirs: Problems, Opportunities and Solutions for Drilling, Completion, Stimulation and Production*", paper SPE 35577 ,presented at the Gas Technology Conference held in Calgary, Alberta April 28 - May 1, 1996.

- 10- Bilu Cherian, Kirk,f, Seth,C. , Conoco,p, Tarik,l. and Malcolm ,Y.,2009,” *Maximizing the Effective Fracture Half-Length to Influence Well Spacing*”, paper SPE 122514,presentd at the 2009 SPE Rocky Mountain Petroleum Technology Conference held in Denver, Colorado, USA, 14–16 April.
- 11- Camacho V.R, R. Raghavan, R. and Reynolds, A., 1987, “*Response of Wells producing layered Reservoirs: Unequal Fracture Length*”; SPEFE pp 9-28 March.
- 12- Cipolla ,C.L., Lolon,E.P., and Mayerhofer, M.J.,2008,”*Resolving Created, Propped, and Effective Hydraulic Fracture Length*”, paper IPTC 12147 ,prepared for presentation at the International Petroleum Technology Conference held in Kuala Lumpur, Malaysia, 3-5 December.
- 13- Crafton, J.W. and Anderson, D.,2006, "*Use of Extremely High Time-Resolution Production Data to Characterize Hydraulic Fracture Properties*", paper SPE 103591, presented at the SPE Annual Technical Conference and Exhibition, San Antonio, Texas, 24-27 September.
- 14- Dariush Malekzadeh, Faid U. Khan, and John J. Day,1995, “*Effective Hydraulic Fracture Length and the Determination of Productivity Index*”,paper SPE 29502, this paper was prepared for presentation at the Production Operations Symposium held in Oklahoma City, OK, U.S.A., 2-4 April.
- 15- Economides, M.J., Oligney, R.E., Valkó.,2002,“*Unified Fracture Design*”,Orsa Press, Houston.
- 16- Elbel, J. and Ayoub, J., 1992, "*Evaluation of Apparent Fracture Lengths Indicated from Transient Tests*", JPT (December) 41-46.
- 17- Elyezer P. Lolon, , Duane A. McVay, and Stephen K. Schubarth,2003,” *Effect of Fracture Conductivity on Effective Fracture Length*”, paper SPE 84311, presented at the SPE Annual Technical Conference and Exhibition held in Denver, Colorado, U.S.A., 5 - 8 October.
- 18- Eric H. Tudor, Grant W. Nevison, and Sean Allen,2009,” *Case Study of a Novel Hydraulic Fracturing Method that Maximizes Effective Hydraulic Fracture Length*”, paper SPE 124480, presented at the SPE Annual Technical Conference and Exhibition held in New Orleans, Louisiana, USA, 4-7 October.
- 19- Gardner, D.C., Hager, C.J., and Agarwal, R.G., 2000, “*Incorporating Rate Time Superposition Into Decline Type Curve Analysis*”, paper SPE 62475, presented

- at the SPE Rocky Mountain Regional Meeting/Low Permeability Reservoirs Symposium, Denver, 12–15 March.
- 20- Hall, H.R., and Yarborough, L., 1973, '*A new equation of state for Z-factor calculations*,' OGI (June 18, 1973).
- 21- Holditch, S. A., Bogatchev, K. Y., 2008, "*Developing Tight Gas Sand Advisor for Completion and Stimulation in Tight Gas Sand Reservoir Worldwide*", Paper SPE 114195.
- 22- Holditch, S.A., 1979, "*Criteria for propping agent selection*". Dallas, Texas, Norton Co.
- 23- Holditch, S.A., 1978, "*Optimization of Well Spacing and Fracture Length in Low Permeability Gas Reservoirs*" paper SPE 7496, presented at the SPE Annual Technical Conference, Houston, Texas, U.S.A, October 1-3.
- 24- Indriati, S., Wang, X., and Economides, M.J., 2002, "*Adjustment of Hydraulic Fracture Design in Gas-Condensate Wells*", paper SPE 73751, presented at the SPE International Symposium on Formation Damage Control, Lafayette, Louisiana, February 20-21.
- 25- Jack Elbel and Joseph Ayoub, 1992, "*Evaluation of apparent fracture lengths indicated from transient tests*", Journal of Canadian Petroleum Technology, Vol 31, No 10, Dec.
- 26- James L. Hunt and M. Y. Soliman, 1994, "*Reservoir Engineering Aspects of Fracturing High Permeability Formations*", paper SPE 28803, presented at the SPE Asia Pacific Oil & Gas Conference held in Melbourne, Australia 7-10 November.
- 27- Kamath, J., Lee, S.H., Jensen, C.L., Narr, W., and Wu, H., 1998, "*Modeling Fluid Flow in Complex Naturally Fractured Reservoirs*," SPE Paper 39547, the Proceedings of the SPE India Oil and Gas Conference and Exhibition, pp. 399–343.
- 28- Lee, Gonzalez, and Eakin, 1966, '*The Viscosity of Natural Gases*', JPT (August 1966).
- 29- Lee, S.H., Jensen, C.L., and Lough, M.F., 1999, "*An Efficient Finite Difference Model for Flow in a Reservoir with Multiple Length-Scale Fractures*," SPE paper 56752, the Proceedings of the SPE Annual Technical Conference & Exhibition held in Houston, U.S.A., 3-6 October.

- 30- Lee, W.J. and Holditch, S.A.1981, "*Fracture Evaluation with Pressure Transient Tests in Low-Permeability Gas Reservoirs*", JPT (September) 1776-1792.
- 31- Lough, M.F., Lee, S.H. and Kamath, J., 1998, "*An Efficient Boundary Integral Formulation for Flow through Fractured Porous Media*", J.Comp. physics.,pp 462–483.
- 32- Lough, M.F., Lee, S.H., and Kamath, J., 1997, "*A New Method to Calculate Effective Permeability of Gridblocks Used in the Simulation of Naturally Fractured Reservoirs*,"SPE Res.Eng. pp. 219–224.
- 33- M.A. Parker, Sanjay Vitthal, Al Rahimi, J.M. McGowan and W.E. Martch Jr., 1994, "*Hydraulic Fracturing of High-Permeability Formations to Overcome Damage*", paper SPE 27378, presented at the SPE Intl. Symposium on Formation Damage Control held in Lafayette, Louisiana, 7-10 February 1994.
- McCain, W. D., Jr., 1990, '*The Properties of Petroleum Fluids*', 2nd Ed.
Penn Well Books, Tulsa.
- 34- Meehan, D.N, 1980, '*Estimating Water Viscosity at Reservoir Conditions*,' Pet. Eng. Int., (July 1980) 117-118.
- 35- Meehan N. ,Horne R. N and Aziz K., 1988, "*Effects of Reservoir Heterogeneity and Fracture Azimuth on Optimization of Fracture Length and Well Spacing*" ,SPE 17606, presented at SPE International Meeting on Petroleum Engineering, held in Tianjin, China, November 1-4.
- 36- Mohan, J,2006, "*Modeling of Gas Condensate Wells with and without Hydraulic Fractures*", MS Thesis, the University of Texas at Austin, August.
- 37- Mohan, J., Sharma, M.M. and Pope, G.A., 2006,"*Optimization of Fracture Length in Gas/Condensate Reservoirs*",paper was prepared for presentation at the 2006 SPE Gas Technology Symposium held in Calgary, Alberta, Canada, 15-17 May 2006.
- 38- Peaceman, D.W., 1983,"*Interpretation of Well-Block Pressures in Numerical Reservoir Simulation with Non-Square Grid Blocks and Anisotropic Permeability*," SPEJ, June, 531-543.
- 39- Piper, McCain & Corredor (1993) gas gravity Piper, L.D., McCain, W.D., Jr., and Corredor, J.H: '*Compressibility Factors for Naturally Occurring Petroleum Gases*,' paper SPE 26668 presented at the 1993 SPE ATCE; SPE Reprint Series No. 52 (1999).

- 40- Poe, B.D, Conger, J.G., 2000, “*Comprehensive Evaluation of Fractured Gas Wells Utilizing Production Data*”, paper 60285, presented at the SPE Rocky Mountain Regional/Low Permeability Reservoir Symposium held in Denver England, CO 12-15 March.
- 41- Pope, G.A., Wu, W., Narayanaswamy G., Delshad, M., and Sharma, M.M., Wang, P., 1998, “*Modeling Relative Permeability Effects in Gas-Condensate Reservoirs*”, paper SPE 49266, presented at the SPE Annual Technical Conference, New Orleans, Louisiana, september 27-30.
- 42- Pridie, David J., 2009, “*Conversations on PTA and Well Testing*”.
- Rushing, J.A. and Blasingame, T.A., 2003, “*Integrating Short-Term Pressure Buildup Testing and Long-Term Production Data Analysis to Evaluate Hydraulically-Fractured Gas Well Performance*” ,paper SPE 84475, presented at the SPE Annual Technical Conference and Exhibition, Denver, Colorado, 5-8 October.
- 43- Spivey, J.P., Valkó, P.P., and McCain, W.D., Jr., 2003, ‘*Coefficients of Isothermal Compressibility of Oilfield Fluid Systems*’ ,unpublished.
Schlumberger, 2013, “*Oil field review summer*”, <Slb.com>.
- 44- Smith, M.B., 2004, “*An Investigation of Non-Darcy Flow Effects on Hydraulic Fractured Oil and Gas Well Performance*”, paper SPE 90864, presented at the 2004 SPE Annual Technical Conference and Exhibition, Houston, Texas, 26-29 September.
- 45- Smith, M.B., Miller, W.K and Haga, J., 1987, “*Tip Screen out Fracturing a Technique for Soft Unstable Formations*”, SPEPE, May, pp95-103.
- 46- Wei, Y. N., And Holditch, S. A., 2009, “*Computing Estimated Values of Optimal Fracture Half Length in the Tight Gas Sand Advisor Program*”, paper SPE 119374, presented at the SPE Hydraulic Fracturing Technology Conference held in The Woodlands, Texas, USA, 19-21 January.
- 47- Xiong, H., 1992, “*Stimex-An Expert System Approach to Well Stimulation.*”, PhD Dissertation, Texas A&M University, College Station, TX.
- 48- Xiong, H., 1993, “*Stimulation Expert Rules Notebook*,” S. A Holditch & Associations, Inc. October.